THE EUROPEAN
PHYSICAL JOURNAL C

Regular Article - Experimental Physics

Search for vector-like quarks in events with two oppositely charged leptons and jets in proton–proton collisions at $\sqrt{s} = 13\,\text{TeV}$

CMS Collaboration[*]

CERN, 1211 Geneva 23, Switzerland

Abstract A search for the pair production of heavy vector-like partners T and B of the top and bottom quarks has been performed by the CMS experiment at the CERN LHC using proton–proton collisions at $\sqrt{s} = 13\,\text{TeV}$. The data sample was collected in 2016 and corresponds to an integrated luminosity of $35.9\,\text{fb}^{-1}$. Final states studied for $\text{T}\overline{\text{T}}$ production include those where one of the T quarks decays via $\text{T} \to \text{tZ}$ and the other via $\text{T} \to \text{bW}$, tZ, or tH, where H is a Higgs boson. For the $\text{B}\overline{\text{B}}$ case, final states include those where one of the B quarks decays via $\text{B} \to \text{bZ}$ and the other $\text{B} \to \text{tW}$, bZ, or bH. Events with two oppositely charged electrons or muons, consistent with coming from the decay of a Z boson, and jets are investigated. The number of observed events is consistent with standard model background estimations. Lower limits at 95% confidence level are placed on the masses of the T and B quarks for a range of branching fractions. Assuming 100% branching fractions for $\text{T} \to \text{tZ}$, and $\text{B} \to \text{bZ}$, T and B quark mass values below 1280 and 1130 GeV, respectively, are excluded.

1 Introduction

The standard model (SM) has been outstandingly successful in describing a wide range of fundamental phenomena. However, one of its notable shortcomings is that it does not provide a natural explanation for the Higgs boson (H) [1–3] observed at 125 GeV [4,5] having a mass that is comparable to the electroweak scale. The suppression of divergent loop corrections to the Higgs boson mass requires either fine-tuning of the SM parameters or new particles at the TeV scale. Many theories of beyond-the-SM physics phenomena that attempt to solve this hierarchy problem predict new particles, which could be partners of the top and bottom quarks and thus cancel the leading loop corrections. Vector-like quarks (VLQs) represent one class of such particles among those that have fermionic properties. Their left- and right-handed components transform in the same way under the SM symmetry

group $\text{SU}(3)_\text{C} \times \text{SU}(2)_\text{L} \times \text{U}(1)_\text{Y}$ [6]. This property allows them to have a gauge-invariant mass term in the Lagrangian of the form $\overline{\psi}\psi$, where ψ represents the fermion field; hence, their masses are not determined by their Yukawa couplings to the Higgs boson. These quarks are not ruled out by the measured properties of the Higgs boson. They are predicted in many beyond-the-SM scenarios such as grand unified theories [7], beautiful mirrors [8], models with extra dimensions [9], little Higgs [10–12], and composite Higgs models [13], as well as theories proposed to explain the SM flavor structure [14] and solve the strong CP problem [15].

The VLQs can be produced singly or in pairs [6]. The cross section for single-quark production is model dependent and depends on the couplings of the VLQs to the SM quarks. On the other hand, pair production of VLQs occurs via the strong interaction, and its cross section is uniquely determined by the mass of the VLQ. Another characteristic of the VLQs is their flavor-changing neutral current decay, which distinguishes them from chiral fermions. The top and bottom quark VLQ partners T and B are expected to couple to the SM third-generation quarks [16], and decay via $\text{T} \to \text{bW}$, tZ, tH and $\text{B} \to \text{tW}$, bZ, bH, respectively.

In this paper, a search for the production of $\text{T}\overline{\text{T}}$ and $\text{B}\overline{\text{B}}$ is presented, where at least one of the T (B) quarks decays as $\text{T} \to \text{tZ}$ ($\text{B} \to \text{bZ}$), as shown in Fig. 1. The search is performed using events with two oppositely charged electrons or muons, consistent with coming from a decay of a Z boson, and jets. The data were collected with the CMS detector at the CERN LHC in 2016, from proton–proton (pp) collisions at $\sqrt{s} = 13\,\text{TeV}$, corresponding to an integrated luminosity of $35.9\,\text{fb}^{-1}$.

Searches for the pair production of T and B quarks have previously been reported by the ATLAS [17–20] and CMS [21–23] Collaborations. The strictest lower limits on the T and B quark masses range between 790 and 1350 GeV, depending on the decay mode studied. The mass range for the T and B quarks studied in this analysis is 800–1500 GeV.

[*] e-mail: cms-publication-committee-chair@cern.ch
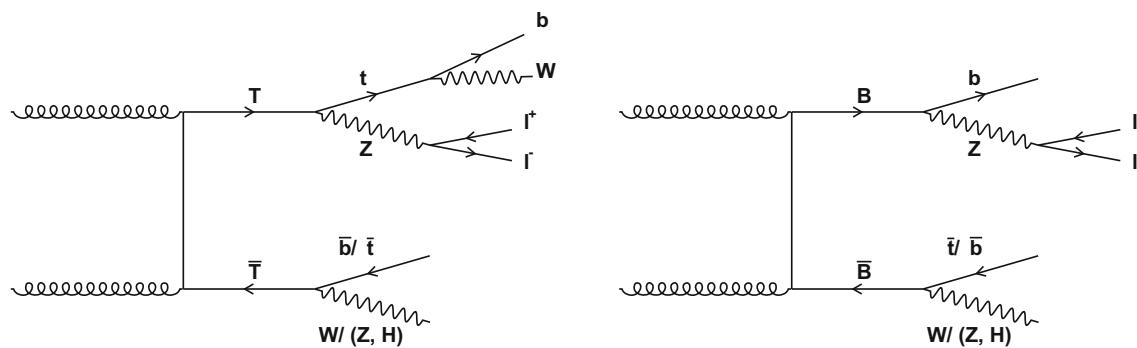
Fig. 1 Leading-order Feynman diagrams for the pair production and decay of T (left) and B (right) VLQs relevant to final states considered in this analysis

2 The CMS detector and event simulation

The central feature of the CMS apparatus is a superconducting solenoid of 6 m internal diameter, providing a magnetic field of 3.8 T. Within the solenoid volume are a silicon pixel and strip tracker, a lead tungstate crystal electromagnetic calorimeter (ECAL), and a brass and scintillator hadron calorimeter (HCAL), each composed of a barrel and two endcap sections. Forward calorimeters extend the pseudorapidity (η) coverage provided by the barrel and endcap detectors. Muons are detected in gas-ionization chambers embedded in the steel flux-return yoke outside the solenoid. A more detailed description of the CMS detector, together with a definition of the coordinate system used and the relevant kinematic variables, can be found in Ref. [24].

Events of interest are selected using a two-tiered trigger system [25]. The first level, composed of custom hardware processors, uses information from the calorimeters and muon detectors to select events at a rate of around 100 kHz within a time interval of less than 4 µs. The second level, known as the high-level trigger, consists of a farm of processors running a version of the full event reconstruction software optimized for fast processing, and reduces the event rate to around 1 kHz before data storage.

Monte Carlo (MC) simulated signal events of the processes pp → T$\overline{\mathrm{T}}$ and pp → B$\overline{\mathrm{B}}$ for T and B quark masses in the range 0.8–1.5 TeV are produced in steps of 0.1 TeV. The events are generated with MadGraph5_aMC@nlo 2.3.3 [26], where the processes are produced at leading order (LO) with up to two partons in the matrix element calculations, using the NNPDF3.0 parton distribution function (PDF) set [27]. Showering and hadronization is simulated with Pythia 8.212 [28] using the underlying event tune CUETP8M1 [29]. To normalize the simulated signal samples to the data, next-to-next-to-leading-order (NNLO) and next-to-next-to-leading-logarithmic (NNLL) soft-gluon resummation cross sections are obtained using the Top++

program (v.2.0) [30], with the MSTW2008NNLO68CL PDF set as implemented in the LHAPDF (v.5.9.0) framework [31].

The main background process is Drell–Yan (Z/γ^*)+jets production, with smaller contributions from t$\overline{\mathrm{t}}$+jets and t$\overline{\mathrm{t}}$Z. Throughout the paper this background will be referred to as DY+jets. Other backgrounds, such as diboson, tZq, tWZ, and t$\overline{\mathrm{t}}$W production, are considerably smaller. The DY+jets simulated background samples are generated in different bins of the Z boson transverse momentum p_T, using the MC@nlo [32] event generator at NLO precision with the FxFx jet-matching scheme [33]. The t$\overline{\mathrm{t}}$+jets events are generated using the Powheg 2.0 [34–36] generator. The generated events are interfaced with Pythia 8.212 [28] for shower modeling and hadronization, using the underlying event tune CUETP8M2T4 [37] for t$\overline{\mathrm{t}}$+jets simulation and CUETP8M1 [29] for the DY+jets process. The SM diboson events are also produced using the same standalone Pythia 8.212 generator. The production of rare single top processes tZq and tWZ, as well as a t$\overline{\mathrm{t}}$ pair in association with a W or Z boson, are simulated with up to one additional parton in the matrix element calculations using the MadGraph5_aMC@nlo 2.3.3 [26] generator at LO precision and matched with the parton showering predictions using the MLM matching scheme [38].

Backgrounds are normalized according to the theoretical predictions for the corresponding cross sections. The DY+jets production cross sections from the MC@nlo [32] generator are valid up to NLO. Using a top quark mass of 172.5 GeV, the t$\overline{\mathrm{t}}$+jets production cross section at NNLO [30] is determined. Diboson production is calculated at NLO for WZ [39] and NNLO for ZZ [40] and WW [41]. The production cross sections for the rare processes tZq, tWZ, and t$\overline{\mathrm{t}}$W are calculated at NLO [42].

A Geant4-based [43,44] simulation of the CMS apparatus is used to model the detector response, followed by event reconstruction using the same software configuration as for the collision data. The effect of additional pp interactions in the same or nearby bunch crossings (pileup) in concurrence

with the hard scattering interaction is simulated using the PYTHIA 8.1 generator and a total inelastic pp cross section of 69.2 mb [42]. The frequency distribution of the additional events is adjusted to match that observed in data and has a mean of 23.

3 Event reconstruction

The event reconstruction in CMS uses a particle-flow (PF) algorithm [45] to reconstruct a set of physics objects (charged and neutral hadrons, electrons, muons, and photons) using an optimized combination of information from the subdetectors. The energy calibration is performed separately for each particle type.

The pp interaction vertices are reconstructed from tracks in the silicon tracker using the deterministic annealing filter algorithm [46]. The pp interaction vertex with the highest $\sum p_T^2$ of the associated clusters of physics objects is considered to be the primary vertex associated with the hard scattering interaction. Here, the physics objects are the jets, which are clustered with the tracks assigned to the vertex using the anti-k_T jet clustering algorithm [47,48], and the missing transverse momentum $\vec{p}_T^{miss}$, defined as the negative vector sum of the $\vec{p}_T$ of those jets, with its magnitude referred to as p_T^{miss}. The interaction vertices not associated with the hard scattering are designated as pileup vertices.

Electron candidates are reconstructed from clusters of energy deposited in the ECAL and from hits in the silicon tracker [49]. The clusters are first matched to track seeds in the pixel detector, then the trajectory of an electron candidate is reconstructed considering energy lost by the electron due to bremsstrahlung as it traverses the material of the tracker, using a Gaussian sum filter algorithm. The PF algorithm further distinguishes electrons from charged pions using a multivariate approach [50]. Observables related to the energy and geometrical matching between track and ECAL cluster(s) are used as main inputs. Additional requirements are applied on the ECAL shower shape, the variables related to the track-cluster matching, the impact parameter, and the ratio of the energies measured in the HCAL and ECAL in the region around the electron candidate. With these requirements, the reconstruction and identification efficiency of an electron from a $Z \to e^+e^-$ decay is on average 70%, whereas the misidentification rate is 1–2% [49]. Electrons with $p_T > 25$ GeV and $|\eta| < 2.4$ are selected for this analysis. Further, electrons passing through the transition regions between the ECAL barrel and endcap sections, $(1.444 < |\eta| < 1.566)$, which are less well measured, are removed.

Muon candidates are identified by multiple reconstruction algorithms using hits in the silicon tracker and signals in the muon system. The standalone muon algorithm uses only information from the muon detectors. The tracker muon algorithm starts from tracks found in the silicon tracker and then associates them with matching tracks in the muon detectors. The global muon algorithm starts from standalone muons and then performs a global fit to consistent hits in the tracker and the muon system [51]. Global muons are used by the PF algorithm. Muons are required to pass additional identification criteria based on the track impact parameter, the quality of the track reconstruction, and the number of hits recorded in the tracker and the muon systems. Muons selected for this analysis are required to have $p_T > 25$ GeV and $|\eta| < 2.4$.

Charged leptons (electrons or muons) from $Z \to e^+e^-$ or $Z \to \mu^+\mu^-$ decays, with the Z boson originating from the decay of a heavy VLQ, are expected to be isolated, i.e., to have low levels of energy deposited in the calorimeter regions around their trajectories. An isolation variable is defined as the scalar p_T sum of the charged and neutral hadrons and photons in a cone centered on the direction of the lepton, of radius $\Delta R \equiv \sqrt{(\Delta \eta)^2 + (\Delta \phi)^2}$, with $\Delta R = 0.3$ (0.4) for electrons (muons). The p_T contributions from pileup and from the lepton itself are subtracted from the isolation variable [49,51]. The relative isolation parameter, defined as the isolation variable divided by the lepton p_T, is required to be less than 0.06 (0.15) for the electrons (muons), with corresponding efficiencies of 85 and 95%, respectively, based on simulation. The isolation requirement helps reject jets misidentified as leptons and reduce multijet backgrounds.

The anti-k_T jet clustering algorithm [47,48] reconstructs jets with PF candidates as inputs. The energy of charged hadrons is determined from a combination of their momentum measured in the tracker and the matching ECAL and HCAL energy deposits, corrected for zero-suppression effects and for the response function of the calorimeters to hadronic showers. Finally, the energy of neutral hadrons is obtained from the corresponding corrected ECAL and HCAL energies. To suppress the contribution from pileup, charged particles not originating from the primary vertex are removed from the jet clustering. An event-by-event jet-area-based correction [52,53] is applied to subtract the contribution of the neutral-particle component of the pileup. Residual corrections are applied to the data to account for the differences with the simulations [54].

Two types of jet are considered, distinguished by the choice of distance parameter used for clustering. Those clustered with a distance parameter of 0.4 ("AK4 jets"), are required to have $p_T > 30$ GeV, and those clustered with a value of 0.8 for this parameter ("AK8 jets") must satisfy the condition $p_T > 200$ GeV, where the jet momentum is the vector sum of the momenta of all particles clustered in the jet. Both classes of jets must satisfy $|\eta| < 2.4$. A new value for p_T^{miss} is determined using the PF objects and including the jet energy corrections.

The combined secondary vertex b tagging algorithm (CSVv2) [55] is used to identify jets originating from the hadronization of b quarks. The algorithm combines information on tracks from the silicon tracker and vertices associated with the jets using a multivariate discriminant. An AK4 jet is defined as a b-tagged jet if the corresponding CSVv2 discriminant is above a threshold that gives an average efficiency of about 70% for b quark jets and a misidentification rate of 1% for light-flavored jets.

The signal events searched for in this analysis have two massive VLQs decaying to at least one Z boson and either a Z, W, or Higgs boson and two heavy quarks. One Z boson must decay leptonically, whereas the remaining Z, W, or Higgs boson is reconstructed using its hadronic decays into jets. Depending on the mass of the VLQ, the decay products can have a large Lorentz boost. In this case, the decay products of $W \to q\bar{q}'$ and $Z \to q\bar{q}$ (collectively labeled as $V \to q\bar{q}$), $H \to b\bar{b}$, and $t \to q\bar{q}'b$ may be contained within a single AK8 jet. These decays are reconstructed using a jet substructure tagger. The decay products of heavy bosons and top quarks that do not acquire a large Lorentz boost are identified by a resolved tagger using AK4 jets. Both types of taggers are described in the next section.

4 Event selection and categorization

For the dielectron ($Z \to e^+e^-$) channel, event candidates are selected using triggers requiring the presence of at least one electron with $p_T > 115\,\text{GeV}$ or a photon with $p_T > 175\,\text{GeV}$. After passing one of the triggers, the triggering electron is also required to pass a set of criteria based on the electromagnetic shower shape and the quality of the electron track. A loose isolation criterion on the electrons is further required, as described in Sect. 3. One of the electrons is required to have $p_T > 120\,\text{GeV}$ in order to remain above the triggering electron p_T threshold. Since the signal electrons originate from the decay of highly boosted Z bosons, these selection criteria preserve the high signal efficiency, while reducing the number of misidentified electrons. The photon trigger helps to retain electrons with $p_T > 300\,\text{GeV}$ that would otherwise be lost because of the requirements on electromagnetic shower shape in the ECAL.

For the dimuon ($Z \to \mu^+\mu^-$) channel, event candidates are selected using a trigger that requires presence of at least one muon with $p_T > 24\,\text{GeV}$. The trigger implements a loose isolation requirement by allowing only a small energy deposit in the calorimeters around the muon trajectory. After passing the trigger, one of the muons from the $Z \to \mu^+\mu^-$ decay must have $p_T > 45\,\text{GeV}$, which provides the largest background rejection that can be obtained without decreasing the signal efficiency for the VLQ mass range of interest. The trigger and lepton reconstruction and identification efficien-

Table 1 Event selection criteria

Variable	Selection
$Z \to \ell\ell$ candidate multiplicity	$= 1$
$p_T(Z)$	$> 100\,\text{GeV}$
AK4 jet multiplicity	≥ 3
H_T	$> 200\,\text{GeV}$
p_T of leading AK4 jet	$> 100\,\text{GeV}$
p_T of subleading AK4 jet	$> 50\,\text{GeV}$
b-tagged AK4 jet multiplicity	≥ 1
p_T of b jet	$> 50\,\text{GeV}$
S_T	$> 1000\,\text{GeV}$

cies are determined using a tag-and-probe method [56]. Scale factors are applied to the simulated events to account for any efficiency differences between the data and simulation.

The invariant mass of the lepton pair from the Z boson leptonic decay must satisfy $75 < m(\ell\ell) < 105\,\text{GeV}$, to be consistent with the Z boson mass, and have a total $p_T(\ell\ell) > 100\,\text{GeV}$, appropriate for the decay of a massive VLQ. Events must have exactly one e^+e^- or $\mu^+\mu^-$ pair candidate consistent with a Z boson decay.

Events are required to have at least three AK4 jets with $H_T > 200\,\text{GeV}$, and $H_T \equiv \sum p_T$, where the summation is over all jets in the event. The highest p_T (leading) AK4 jet is required to have $p_T > 100\,\text{GeV}$, the second-highest-p_T (subleading) AK4 jet to have $p_T > 50\,\text{GeV}$, and all other jets must satisfy the condition $p_T > 30\,\text{GeV}$. The AK4 (AK8) jets j within $\Delta R(\ell, j) < 0.4\,(0.8)$ of either lepton from the Z boson decay are not considered further in the analysis. At least one b-tagged jet with $p_T > 50\,\text{GeV}$ is required. The S_T variable, defined as the sum of H_T, $p_T(Z)$, and p_T^{miss}, must be greater than 1000 GeV. The selection criteria are summarized in Table 1. The selections are optimized to obtain the largest suppression of SM backgrounds that can be achieved without reducing the simulated signal efficiency by more than 1%.

The event topologies are different for $T\overline{T}$ and $B\overline{B}$ decays, and the product of the signal efficiency and the acceptance varies from 1.2 to 2.6% over the various signal channels. The $T\overline{T}$ events are characterized by three heavy bosons and two heavy quarks in the decay sequence. The $B\overline{B}$ events have two heavy bosons and two heavy quarks, hence more energetic final decay objects. Therefore, the analysis is optimized separately for the $T\overline{T}$ and $B\overline{B}$ channels.

For both searches the decays of boosted $V \to q\bar{q}$ and $H \to b\bar{b}$ are reconstructed from AK8 jets, using the jet substructure tagger, and are referred to as V and H jets, respectively. As the Higgs boson mass is larger than W and Z boson masses, it requires a higher momentum for its decay products to merge into a single AK8 jet. Therefore, H jets are required to have $p_T > 300\,\text{GeV}$ and V jets have $p_T > 200\,\text{GeV}$. A jet

pruning algorithm [57,58] is used to measure the jet mass. The V and H jet candidates are required to have a pruned jet mass in the range 65–105 and 105–135 GeV, respectively. The jet pruning algorithm reclusters the groomed jets [59] by eliminating low energy subjets subjets. In the subsequent recombination of two subjets, the ratio of the subleading subjet p_T to the pruned jet p_T must be greater than 0.1 and the distance between the two subjets must satisfy $\Delta R < m_{jet}/2p_{T jet}$, where m_{jet} and $p_{T jet}$ are the mass and p_T of the pruned jet, respectively.

The N-subjettiness algorithm [60] is used to calculate the jet shape variable τ_N, which quantifies the consistency of a jet with the hypothesis of the jet having N subjets, each arising from a hard parton coming from the decay of an original heavy boson. The V and H jets in the $T\overline{T}$ ($B\overline{B}$) search are required to have an N-subjettiness ratio $\tau_{21} \equiv \tau_2/\tau_1 < 1.0 (0.6)$. Both pruned subjets coming from the H jet are required to be b-tagged. This is done by using the above-mentioned CSVv2 b-tagging algorithm with a cut that gives a 70–90% efficiency for b quark subjets, depending on the subjet p_T, and a misidentification rate of 10% for subjets from light-flavored quarks and gluons.

Boosted top quarks decaying to bq$\overline{q}'$ are identified ("t tagged") using AK8 jets and the soft-drop algorithm [61,62] to groom the jet. This algorithm recursively declusters a jet into two subjets. It discards soft and wide-angle radiative jet components until a hard-splitting criterion is met, to obtain jets consistent with the decay of a massive particle. We use the algorithm with an angular exponent $\beta = 0$, a soft cutoff threshold $z_{cut} < 0.1$, and a characteristic radius $R_0 = 0.8$. For top quark jets, the soft-drop mass must be in the range 105–220 GeV and the N-subjettiness ratio $\tau_{32} \equiv \tau_3/\tau_2 < 0.81 (0.67)$ for the $T\overline{T}$ ($B\overline{B}$) search, consistent with the expectation for three subjets from top quark decay. There are a total of five heavy bosons and quarks produced in $T\overline{T}$ signal events, whereas there are only four in $B\overline{B}$ events. Thus it is possible to apply a tighter N-subjetiness ratio criterion in the $B\overline{B}$ analysis without a loss of signal efficiency.

Corrections to the jet mass scale, resolution and τ_{21} selection efficiency for V jets due to the difference in data and MC simulation are measured using a sample of semileptonic $t\overline{t}$ events [63]. For the correction to the jet mass scale and resolution, boosted W bosons produced in the top quark decays are separated from the combinatorial $t\overline{t}$ background by performing a simultaneous fit to the observed pruned jet mass spectrum. In order to account for the difference in the jet shower profile of V → q$\overline{q}$ and H → b$\overline{b}$ decays, a correction factor to the H jets mass scale and resolution [64] is measured by comparing the ratio of H and V jet efficiencies using the PYTHIA 8.212 [28] and HERWIG++ [65] shower generators. In addition, the corrections to τ_{21} selection efficiency are obtained based on the difference between data

and simulation [64] for H-tagged jets. All these corrections are propagated to V, top quark and H jets, respectively. For top quark jets, the corrections to the τ_{32} selection efficiency are measured between data and simulation [63] using soft-drop groomed jets. To account for the misidentification of boosted V-, H-, and t-tagged jets in the background samples, mistagging scale factors are derived from a region in the data enriched in Z+jets events, which is constructed using the selection criteria listed in Table 1, with the exception that events must have zero b jets. These mistagging scale factors are applied to the mistagged jets in simulated signal and background events.

In the $T\overline{T}$ search, in addition to the jet substructure techniques, the W, Z, H, and top quark decays are reconstructed with a resolved tagger using AK4 jets, as described below. Only those AK4 jets that are a radial distance $\Delta R > 0.8$ from the tagged AK8 jets are considered in the resolved tagging algorithm. The resolved V → q$\overline{q}$ and H → b$\overline{b}$ candidates are composed of two AK4 jets j_1 and j_2 whose invariant mass must satisfy $70 < m(j_1 j_2) < 120$ GeV and $80 < m(j_1 j_2) < 160$ GeV, respectively, and have $p_T(j_1 j_2) > 100$ GeV. For H candidates, at least one of the jets must be b tagged. The resolved top quark candidate is composed of either three AK4 jets j_1, j_2, and j_3 with an invariant mass $120 < m(j_1 j_2 j_3) < 240$ GeV and $p_T(j_1 j_2 j_3) > 100$ GeV, or an AK4 jet j_1 and an AK8 V jet satisfying $120 < m(V j_1) < 240$ GeV and $p_T(V j_1) > 150$ GeV. These selection criteria are derived from simulated $T\overline{T}$ events, using MC truth information.

The $T\overline{T}$ events are next classified based on the number of AK4 b-tagged jets (N_b), and number of V → q$\overline{q}$ (N_V), H → b$\overline{b}$ (N_H), and t → q$\overline{q}'$b (N_t) candidates identified using either the jet substructure or resolved tagging algorithms. In an event, N_b can be 1 or ≥ 2, and N_V, N_H, and N_t each can be 0 or ≥ 1. Thus, in total, $2 \times 2 \times 2 \times 2 = 16$ categories of events are constructed. For simplicity, overlaps between candidates of different types are allowed, e.g., the same AK8 jet could be tagged as both a top quark and an H candidate because of the overlapping mass windows. Such overlaps occur in a few percent of the signal events. However, by construction each event can belong to only one category. In the example above, the event would fall into a category with both $N_H \geq 1$ and $N_t \geq 1$ requirements satisfied. Further, the mistag rates and the relevant corrections to the jet mass scale and resolution are applied to the H and t candidates, based on MC truth information.

Next, the event categories are sorted using the figure of merit $S/\sqrt{B}$, where S and B are the expected $T\overline{T} \to tZtZ$ signal and background event yields, respectively, as determined from the simulation. The categories with similar figures of merit based on expected upper limits at 95% confidence level (CL) are grouped together, while the categories that are found not to add sensitivity to the $T\overline{T}$ signal are discarded. A total of four event groups labeled A through D are selected, each with

Table 2 The first four columns show different event groups used for the T$\overline{\text{T}}$ search, classified according to the number of b-tagged jets N_b and the number of V $\rightarrow$ q$\overline{\text{q}}$, H $\rightarrow$ b$\overline{\text{b}}$, and t $\rightarrow$ q$\overline{\text{q}}'$b candidates in the event, N_V, N_H and N_t, respectively, identified using both the jet substructure and resolved tagger algorithms. The last three columns show the relative signal acceptance for a T quark of mass 1200 GeV for decay channels tZtZ, tZtH and tZbW as described in text

Group	N_b	N_V	N_H	N_t	tZtZ (%)	tZtH (%)	tZbW (%)
A	= 1	≥ 1	= 0	≥ 1	37.8	27.2	31.9
	= 1	≥ 1	≥ 1	≥ 1			
B	≥ 2	≥ 1	= 0	≥ 1	32.2	42.1	20.6
	≥ 2	≥ 1	≥ 1	≥ 1			
C	= 1	= 0	= 0	≥ 1	8.4	6.6	11.6
	≥ 2	≥ 1	= 0	= 0			
D	≥ 2	≥ 1	≥ 1	= 0	8.7	13.4	8.2
	≥ 2	= 0	≥ 1	≥ 1			
	≥ 2	= 0	= 0	≥ 1			

a different signal acceptance relative to the selection criteria described in Table 1 and depending on the T decay channel. Table 2 shows the selections on these event groups, and the relative signal acceptances of the T quark decay channels, namely, tZtZ, tZtH, or tZbW for a T quark of mass 1200 GeV. The decay channels are defined with a benchmark combination of branching fractions $\mathcal{B}(T \rightarrow tZ) = 100\%$ (tZtZ), $\mathcal{B}(T \rightarrow tZ) = \mathcal{B}(T \rightarrow tH) = 50\%$ (tZtH), and $\mathcal{B}(T \rightarrow tZ) = \mathcal{B}(T \rightarrow bW) = 50\%$ (tZbW). Events from all the decay channels mainly contribute to groups A and B, whereas groups C and D have slightly lower acceptance depending on the decay channel. The fraction of the signal identified by the jet substructure and resolved taggers depends on the T quark mass. For masses below 1200 GeV, the two taggers are equally efficient in identifying signal events for all the channels. For T quark masses above 1200 GeV, the jet substructure tagger becomes more efficient. For example, for T quark mass at 1800 GeV, the jet substructure tagger selects twice as many T quark candidates as the resolved tagger.

Because the event topology of B$\overline{\text{B}}$ signal events is different from that of T$\overline{\text{T}}$ signal events, as discussed previously, the V, H, and t candidates in the B$\overline{\text{B}}$ analysis are identified using only the jet substructure tagger. Events are then separated into five categories, labeled 1b, 2b, boosted t, boosted H, and boosted Z, based on the values of N_b, N_V, N_H, and N_t. Table 3 shows these categories, and the relative signal acceptances of B quark decay channels, namely, bZbZ, bZbH, or bZtW for a B quark of mass 1200 GeV. The decay channels are defined with a benchmark combination of branching fractions $\mathcal{B}(B \rightarrow bZ) = 100\%$ (bZbZ), $\mathcal{B}(B \rightarrow bZ) = \mathcal{B}(B \rightarrow bH) = 50\%$ (bZbH), and $\mathcal{B}(B \rightarrow bZ) = \mathcal{B}(B \rightarrow tW) = 50\%$ (bZtW).

5 Background modeling

The backgrounds from all sources are estimated using simulation, except for Z+jets where corrections to the simulated events are applied using data, as described below. The modeling of simulated background events is validated using several control regions in the data, which are constructed by inverting one or more of the requirements listed in Table 1. The control region labeled CR0b+high-S_T is constructed by requiring zero b jets. The control region CR1b+low-S_T is constructed by inverting the S_T requirement: $S_T \leq 1000$ GeV. The control region CR0b is constructed by requiring zero b jets and removing the S_T requirement. Signal contamination from all channels in each of these control regions is less than 1%.

The AK4 jet multiplicity distribution is not modeled reliably in the Z+jets simulation, and therefore it is corrected using scale factors obtained from data. Scale factors listed in Table 4 are determined using the CR0b control region, which is enriched with Z+jets events. After applying these corrections, the distributions of kinematic variables in the control regions from the background simulations are in agreement with the data, as shown for example in Fig. 2 for the S_T distributions.

Table 3 The first four columns show different event categories used for the B$\overline{\text{B}}$ search, classified according to the number of AK4 b-tagged jets N_b and the number of V $\rightarrow$ q$\overline{\text{q}}$, H $\rightarrow$ b$\overline{\text{b}}$, and t $\rightarrow$ q$\overline{\text{q}}'$b candidates in the event, N_V, N_H, and N_t, respectively, identified using the jet substructure algorithm. The last three columns show the relative signal acceptance for a B quark of mass 1200 GeV for decay channels bZbZ, bZbH and bZtW as described in text

Category	N_b	N_V	N_H	N_t	bZbZ (%)	bZbH (%)	bZtW (%)
1b	= 1	= 0	= 0	= 0	50.4	27.4	22.3
2b	≥ 2	= 0	= 0	= 0	45.7	34.3	20.0
Boosted t	≥ 1	≥ 0	≥ 0	≥ 1	35.1	24.3	40.6
Boosted H	≥ 1	≥ 0	≥ 0	= 0	21.4	64.3	14.3
Boosted Z	≥ 1	≥ 1	= 0	= 0	52.4	21.7	25.9

Table 4 The scale factors determined from data for correcting the AK4 jet multiplicity distribution in the simulation. The quoted uncertainties in the scale factors are statistical only

Number of AK4 jets	Scale factor
3	0.92 ± 0.01
4	1.03 ± 0.01
5	1.12 ± 0.02
6	1.30 ± 0.05
≥ 7	1.61 ± 0.12

6 Systematic uncertainties

The systematic uncertainties in the SM background rates are due to the uncertainties in the CMS measurements of $d\sigma/dH_T$ for Z+jets [66], $d\sigma/dm_{t\bar{t}}$ for $t\bar{t}$+jets [67], and $d\sigma/dp_T(Z)$ for diboson production [68]. They are estimated to be 15% in each case. The measured integrated luminosity uncertainty of 2.5% [69] affects both the signal and background rate predictions. The uncertainties associated with the measured data-to-simulation efficiency scale factors for the lepton identification and the trigger efficiencies are 3 and 1%, respectively.

The effect on the signal and background acceptance uncertainties due to the renormalization and factorization scale (μ_f and μ_r) uncertainties and the PDF choices in the simulations are taken into account in the statistical analysis. The influence of μ_f and μ_r scale uncertainties are estimated by varying the default scales by the following six combinations

of factors, $(\mu_f, \mu_r) \times (1/2, 1/2)$, $(1/2, 1)$, $(1, 1/2)$, $(2, 2)$, $(2, 1)$, and $(1, 2)$. The maximum and minimum of the six variations are computed for each bin of the S_T distribution, producing an uncertainty "envelope". The uncertainties due to the PDF choices in the simulations are estimated using the PDF4LHC procedure [27,70–72], where the root-mean-square of 100 pseudo-experiments provided by the PDF sets represents the uncertainty envelope. The background and signal event counts are then varied relative to their nominal values up and down by a factor of two times the uncertainty envelopes. The impacts of these variations on the background and signal shape are also taken into account. The effect of the μ_f and μ_r scale uncertainties on the $T\bar{T}$ and $B\bar{B}$ signal yield is $< 1\%$. However, this has the largest effect, amounting to as much as 36% on the background yield. The effect due to PDF choices amounts to a 3.2–9.5% change in the signal and background yields. The effect of the uncertainty in the pileup determination is estimated by varying the nominal pp inelastic cross section by 4.6% [42], which has an impact of 1.5–3.6% on the signal yields. Differences between simulation and data in the jet multiplicity distributions in DY+jets background events, derived in the CR0b region as shown in Table 4, are taken as an estimate of the associated systematic uncertainty, which ranges from 4.0–11.5%

Several uncertainties are associated with the measurement of jet-related quantities. The jet energy scale and resolution uncertainties are about 1% [54,73]. The AK8 pruned jet mass scale and resolution uncertainties are evaluated to be 2.3 and 18% [63], respectively. The effect of these uncertainties on the $T\bar{T}$ and $B\bar{B}$ signal yields is 1.5–4.4% and 1.0–
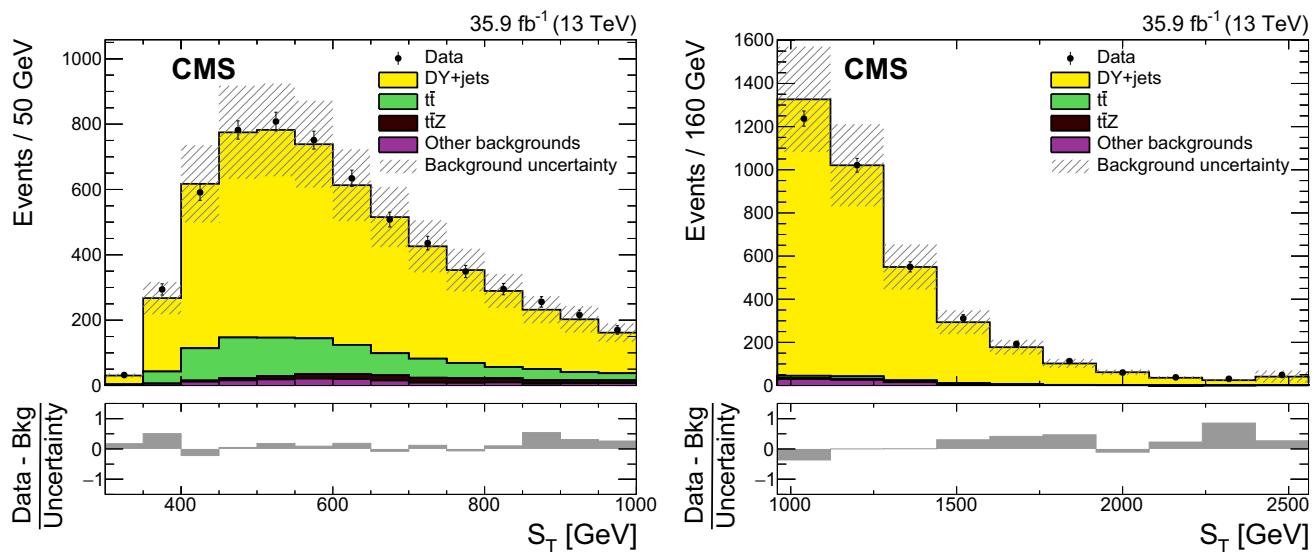

Fig. 2 The S_T distributions for the CR1b+low-S_T (left) and CR0b+high-S_T (right) control regions for the data (points) and the background simulations (shaded histograms) after applying the scale factors given in Table 4. The vertical bars on the points represent the statistical

uncertainties in the data. The hatched bands indicate the total uncertainties in the simulated background contributions added in quadrature. The lower plots show the difference between the data and the simulated background, divided by the total uncertainty

Table 5 Summary of systematic uncertainties considered in the statistical analysis of $T\overline{T}$ and $B\overline{B}$ search on the background and signal events. All uncertainties affect the normalizations of the S_T distributions. The tick mark indicates the uncertainties that also affect the shape, and the uncertainty range accounts for their effects on the expected yields across all the $T\overline{T}$ groups or $B\overline{B}$ categories. The $T\overline{T}$ and $B\overline{B}$ signal events correspond to the benchmark decay channels tZtZ and bZbZ, respectively, for T and B quark mass $m_T = m_B = 1200$ GeV

Source	Shape	Uncertainty (%)			
		$T\overline{T}$		$B\overline{B}$	
		Background yield	Signal yield	Background yield	Signal yield
$t\overline{t}$+jets rate		15	–	15	–
DY+jets rate		15	–	15	–
Diboson rate		15	–	15	–
Integrated luminosity		2.5	2.5	2.5	2.5
Lepton identification		3	3	3	3
Trigger efficiency		1	1	1	1
PDF	✓	4.8–6.6	4.5–7.8	3.2–7.1	4.6–9.5
μ_f and μ_r	✓	12.9–25.8	0.1–0.2	12.7–36.5	0.1–0.4
Pileup	✓	3.5–5.0	1.5–2.6	1.8–6.7	1.8–3.6
DY+Jets correction factor	✓	4.2–11.4	–	1.5–7.8	–
Jet energy scale	✓	5.4–8.2	1.6–4.0	4.9–9.1	3.3–4.4
Jet energy resolution	✓	2.0–3.8	0.6–1.8	3.2–6.7	1.7–3.8
V and H tagging	✓	1.5–2.5	0.3–1.3	0.2–6.3	0.2–8.4
t tagging	✓	0.5–3.0	4.8–7.6	0.2–6.3	0.2–8.4
misidentification of V	✓	0.6–2.3	0.1–0.2	0.3–4.9	0.0–5.3
misidentification of H	✓	0.0–0.7	0.0–0.7	0.0–14.4	0.0–14.4
misidentification of t	✓	1.0–2.3	0.2–0.4	6.8	6.8
b tagging	✓	4.1–6.2	1.0–7.2	8.3–23.6	1.8–10.2

3.8%, respectively. These uncertainties, in addition to the uncertainties in the τ_{21} (8%) and τ_{32} (11%) selections [63], are applied for the V-, H-, and t-tagged jets. The systematic uncertainties due to the jet shower profile differences between the jets in the $W \rightarrow q\overline{q}'$ and $H \rightarrow b\overline{b}$ processes are estimated from the difference observed between results obtained with the PYTHIA 8 and HERWIG++ generators and are applied to the V- and H-tagged jets. The overall effect of V, H, and t tagging uncertainties on $T\overline{T}$ and $B\overline{B}$ signal yields is 0.2–8.4%. The uncertainties in the misidentification rates of boosted jets are 5, 14, and 7% for the W-, H-, and t-tagged jets, respectively. They are used to derive the uncertainties in the estimates of the numbers of mistagged jets in the signal and background simulated events, which result in uncertainties in the $B\overline{B}$ signal yields of up to 14%. The uncertainties in the b tagging efficiency scale factors are propagated to the final result, with the uncertainties in the b- and c-flavored quark jets treated as fully correlated. These uncertainties are in the range 2–5% for b-flavored jets, a factor of two larger for c-flavored jets, and $\approx$10% for light-flavored jets. The uncertainties due to heavy- and light-flavored jets are considered uncorrelated. Table 5 summarizes the systematic uncertainties in the background and signal yields in the $T\overline{T}$ and $B\overline{B}$ searches. The ranges correspond to the impact on event yields

due to systematic uncertainties that affect both the rates and shapes across all the $T\overline{T}$ groups or $B\overline{B}$ categories. Here the $T\overline{T}$ and $B\overline{B}$ signals correspond to the benchmark decay channels tZtZ and bZbZ, respectively, for a T and B quark mass $m_T = m_B = 1200$ GeV.

7 Results

7.1 T quark search

The number of observed events for the $T\overline{T}$ production search in the A, B, C, and D event groups are given for the electron and muon channels in Tables 6 and 7, respectively, along with the numbers of predicted background events. The expected numbers of signal events for T quark masses of 800 and 1200 GeV are also shown in the same tables, for three different decay scenarios, with branching fractions $\mathcal{B}(T \rightarrow tZ) = 100\%$ (tZtZ), $\mathcal{B}(T \rightarrow tZ) = \mathcal{B}(T \rightarrow tH) = 50\%$ (tZtH), and $\mathcal{B}(T \rightarrow tZ) = \mathcal{B}(T \rightarrow bW) = 50\%$ (tZbW). The predicted background and observed event yields agree within their uncertainties.

To determine the upper limits on the $T\overline{T}$ cross section, the electron and muon channels are combined, and a simultane-

Table 6 The number of observed events and the predicted number of SM background events in the T$\overline{\text{T}}$ search using Z $\rightarrow$ e$^+$e$^-$ channel in the four event groups. The expected numbers of signal events for T quark masses of 800 and 1200 GeV for three different decay scenarios with assumed branching fractions $\mathcal{B}(\text{T} \rightarrow \text{tZ}) = 100\%$ (tZtZ) , $\mathcal{B}(\text{T} \rightarrow \text{tZ}) = \mathcal{B}(\text{T} \rightarrow \text{tH}) = 50\%$ (tZtH), and $\mathcal{B}(\text{T} \rightarrow \text{tZ}) = \mathcal{B}(\text{T} \rightarrow \text{bW}) = 50\%$ (tZbW) are also shown. The uncertainties in the number of expected background events include the statistical and systematic uncertainties added in quadrature

Event group		A	B	C	D
DY+jets		54.9 ± 5.2	9.0 ± 1.9	17.0 ± 2.4	7.2 ± 1.4
t$\bar{\text{t}}$+jets		7.9 ± 1.7	1.7 ± 0.8	3.2 ± 1.1	1.8 ± 0.8
t$\bar{\text{t}}$Z		8.2 ± 0.8	4.9 ± 0.6	1.3 ± 0.2	1.3 ± 0.2
Other backgrounds		3.0 ± 1.7	0.9 ± 0.7	0.6 ± 0.4	0.1 ± 0.1
Total		74.1 ± 6.2	16.5 ± 2.5	22.2 ± 2.9	10.4 ± 1.8
Data		84	15	25	11
tZtZ,	$m_\text{T} = 800$ GeV	54.9 ± 2.2	43.6 ± 2.0	9.6 ± 0.9	9.6 ± 0.9
tZtH,	$m_\text{T} = 800$ GeV	24.8 ± 1.0	26.7 ± 0.8	4.2 ± 0.3	6.5 ± 0.4
tZbW,	$m_\text{T} = 800$ GeV	24.5 ± 1.0	17.9 ± 0.6	5.4 ± 0.3	5.2 ± 0.3
tZtZ,	$m_\text{T} = 1200$ GeV	3.6 ± 0.1	3.3 ± 0.1	0.9 ± 0.1	0.8 ± 0.1
tZtH,	$m_\text{T} = 1200$ GeV	1.6 ± 0.1	1.8 ± 0.1	0.4 ± 0.1	0.6 ± 0.1
tZbW,	$m_\text{T} = 1200$ GeV	1.6 ± 0.1	1.3 ± 0.1	0.5 ± 0.1	0.4 ± 0.1

Table 7 The number of observed events and the predicted number of SM background events in the T$\overline{\text{T}}$ search using Z $\rightarrow$ $\mu^+\mu^-$ channel in the four event groups. The expected numbers of signal events for T quark masses of 800 and 1200 GeV for three different decay scenarios with assumed branching fractions $\mathcal{B}(\text{T} \rightarrow \text{tZ}) = 100\%$ (tZtZ) , $\mathcal{B}(\text{T} \rightarrow \text{tZ}) = \mathcal{B}(\text{T} \rightarrow \text{tH}) = 50\%$ (tZtH), and $\mathcal{B}(\text{T} \rightarrow \text{tZ}) = \mathcal{B}(\text{T} \rightarrow \text{bW}) = 50\%$ (tZbW) are also shown. The uncertainties in the number of expected background events include the statistical and systematic uncertainties added in quadrature

Event group		A	B	C	D
DY+jets		102.5 ± 10.2	15.8 ± 3.1	36.8 ± 4.4	10.2 ± 2.1
t$\bar{\text{t}}$+jets		18.4 ± 3.4	6.8 ± 1.7	5.7 ± 1.5	6.3 ± 1.7
t$\bar{\text{t}}$Z		12.5 ± 1.2	7.7 ± 1.0	2.0 ± 0.3	2.3 ± 0.3
Other backgrounds		4.2 ± 1.3	0.9 ± 0.4	0.5 ± 0.3	0.3 ± 0.1
Total		137.6 ± 11.6	31.2 ± 4.5	45.0 ± 5.0	19.1 ± 3.2
Data		126	36	45	22
tZtZ,	$m_\text{T} = 800$ GeV	72.8 ± 2.5	65.4 ± 2.4	10.9 ± 1.0	11.9 ± 1.0
tZtH,	$m_\text{T} = 800$ GeV	33.0 ± 0.8	40.0 ± 0.9	5.5 ± 0.3	8.4 ± 0.4
tZbW,	$m_\text{T} = 800$ GeV	34.9 ± 0.9	26.2 ± 0.8	7.0 ± 0.4	7.0 ± 0.4
tZtZ,	$m_\text{T} = 1200$ GeV	4.4 ± 0.1	3.7 ± 0.1	1.2 ± 0.1	1.0 ± 0.1
tZtH,	$m_\text{T} = 1200$ GeV	2.0 ± 0.1	2.2 ± 0.1	0.6 ± 0.1	0.8 ± 0.1
tZbW,	$m_\text{T} = 1200$ GeV	1.9 ± 0.1	1.4 ± 0.1	0.7 ± 0.1	0.5 ± 0.1

ous binned maximum-likelihood fit is performed on the S_T distributions in data for the four event groups. The measured S_T distributions in data are shown in Fig. 3 for each of the event groups, along with the predicted background distributions and the expected signal distributions for T$\overline{\text{T}} \rightarrow$ tZtZ with $m_\text{T} = 1200$ GeV. The impact of the statistical uncertainty in the simulated samples is reduced by rebinning each S_T distribution to ensure that the statistical uncertainty associated with the expected background is less than 20% in each bin. There is no indication of a signal in the S_T distribution of any of the event groups.

The upper limits at 95% CL on the T$\overline{\text{T}}$ cross section are computed using a Bayesian likelihood-based technique [74] with the THETA framework [75]. All the systematic uncertainties due to normalization variations described in the previous section enter the likelihood as nuisance parameters with log-normal prior distributions, whereas the uncertainties from the shape variations are assigned Gaussian-distributed priors. For the signal cross section parameter, we use a uniform prior distribution. The likelihood is marginalized with respect to the nuisance parameters, and the limits are
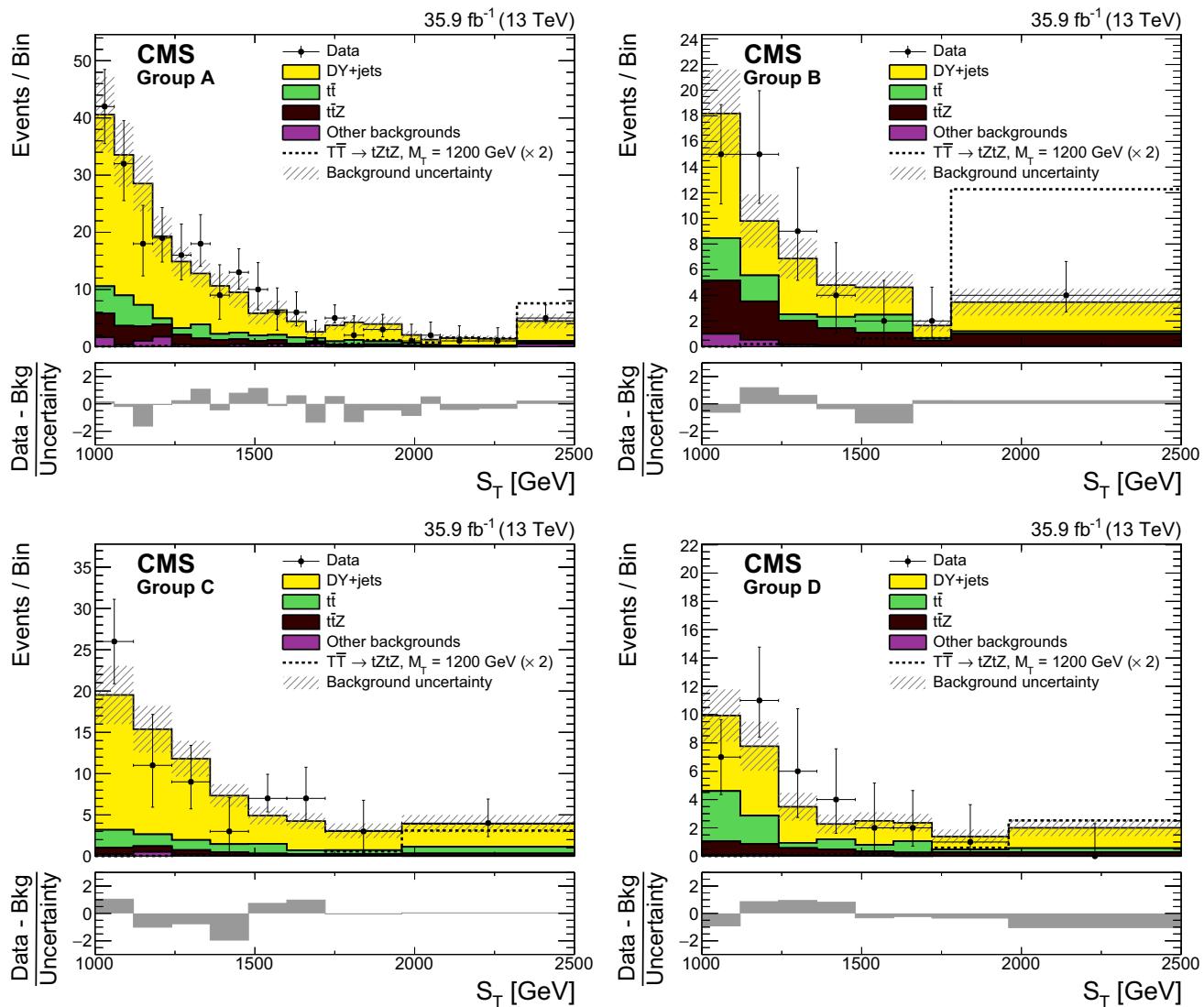
Fig. 3 The S_T distributions for groups A, B, C, D (left to right, upper to lower) from data (points with vertical and horizontal bars), the expected SM backgrounds (shaded histograms), and the expected signal, scaled up by a factor 2, for $T\overline{T} \rightarrow tZtZ$ with $m_T = 1200\,\mathrm{GeV}$ (dotted lines). The vertical bars on the points show the central 68% CL intervals for Poisson-distributed data. The horizontal bars give the bin widths. The hatched bands represent the statistical and systematic uncertainties in the total background contribution added in quadrature. The lower plots give the difference between the data and the total expected background, divided by the total background uncertainty

extracted from a simultaneous maximum-likelihood fit of the S_T distributions in all four groups shown in Fig. 3.

The upper limits on the $T\overline{T}$ cross section are computed for different T quark mass values and for the three branching fraction scenarios listed above. The upper limits at 95% CL on the $T\overline{T}$ cross section are shown as a function of the T quark mass by the solid line in Fig. 4. The median expected upper limit is given by the dotted line, while the inner and outer bands correspond to one and two standard deviation uncertainties, respectively, in the expected limit. The dotted-dashed curve displays the predicted theoretical signal cross section [30]. Comparing the observed cross section limits to the theoretical signal cross section, we exclude T quarks with masses less than 1280, 1185, and 1120 GeV, respectively, for the three branching ratio hypotheses listed above. The expected upper limits are 1290, 1175, and 1115 GeV for the respective scenarios.

Figure 5 (upper) displays the observed (left) and expected (right) 95% CL lower limits on the T quark mass as a function of the relevant branching fractions, assuming $\mathcal{B}(T \rightarrow tZ) + \mathcal{B}(T \rightarrow tH) + \mathcal{B}(T \rightarrow bW) = 1.0$. For a T quark decaying exclusively via $T \rightarrow tZ$, the lower mass limit is 1280 GeV.
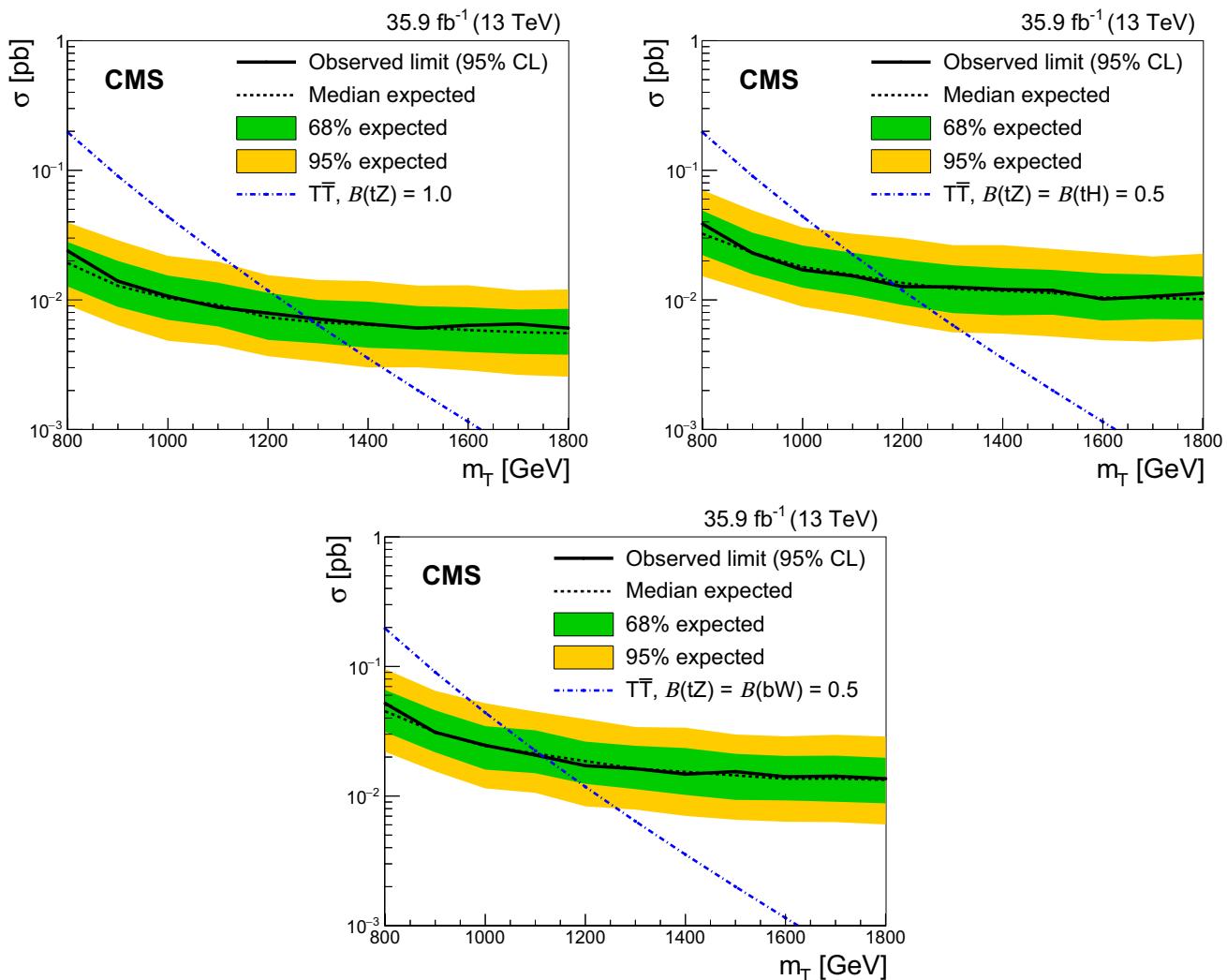
Fig. 4 The observed (solid line) and expected (dashed line) 95% CL upper limits on the $T\overline{T}$ cross section as a function of the T quark mass assuming (upper left) $\mathcal{B}(T \to tZ) = 100\%$, (upper right) $\mathcal{B}(T \to tZ) = \mathcal{B}(T \to tH) = 50\%$, and (lower) $\mathcal{B}(T \to tZ) = \mathcal{B}(T \to bW) = 50\%$.

The dotted-dashed curve displays the theoretical $T\overline{T}$ production cross section. The inner and outer bands show the one and two standard deviation uncertainties in the expected limits, respectively

7.2 B quark search

The numbers of observed and predicted background events in the five event categories for the $B\overline{B}$ search using $Z \to e^+e^-$ and $Z \to \mu^+\mu^-$ are given in Tables 8 and 9, respectively. The expected number of signal events in each category is also shown for B masses of 800 and 1200 GeV. The branching fraction hypotheses assumed for the three decay channels are $\mathcal{B}(B \to bZ) = 100\%$ (bZbZ), $\mathcal{B}(B \to bZ) = \mathcal{B}(B \to bH) = 50\%$ (bZbH), and $\mathcal{B}(B \to bZ) = \mathcal{B}(B \to tW) = 50\%$ (bZtW). The numbers of observed and expected background events are consistent with each other for every event category. As with the $T\overline{T}$ search, 95% CL upper limits on the $B\overline{B}$ production cross section are determined using a simultaneous binned maximum-likelihood fit to the S_T

distributions for the different event categories, shown in Fig. 6.

The upper limits at 95% CL on the $B\overline{B}$ cross section are shown by the solid line in Fig. 7. As before, the inner and outer bands give the one and two standard deviation uncertainties, respectively, in the expected upper limits. The dotted curve displays the theoretical signal cross section. Comparing the observed cross section limits to the signal cross section, we exclude B quarks with masses less than 1130, 1015, and 975 GeV in the bZbZ, bZbH, and bZtW channels, respectively. The corresponding expected values are 1200, 1085, and 1055 GeV.

Figure 5 (lower) displays the observed (left) and expected (right) 95% CL lower limits on the B quark mass as a function of the relevant branching fractions, assuming $\mathcal{B}(B \to bZ) +$
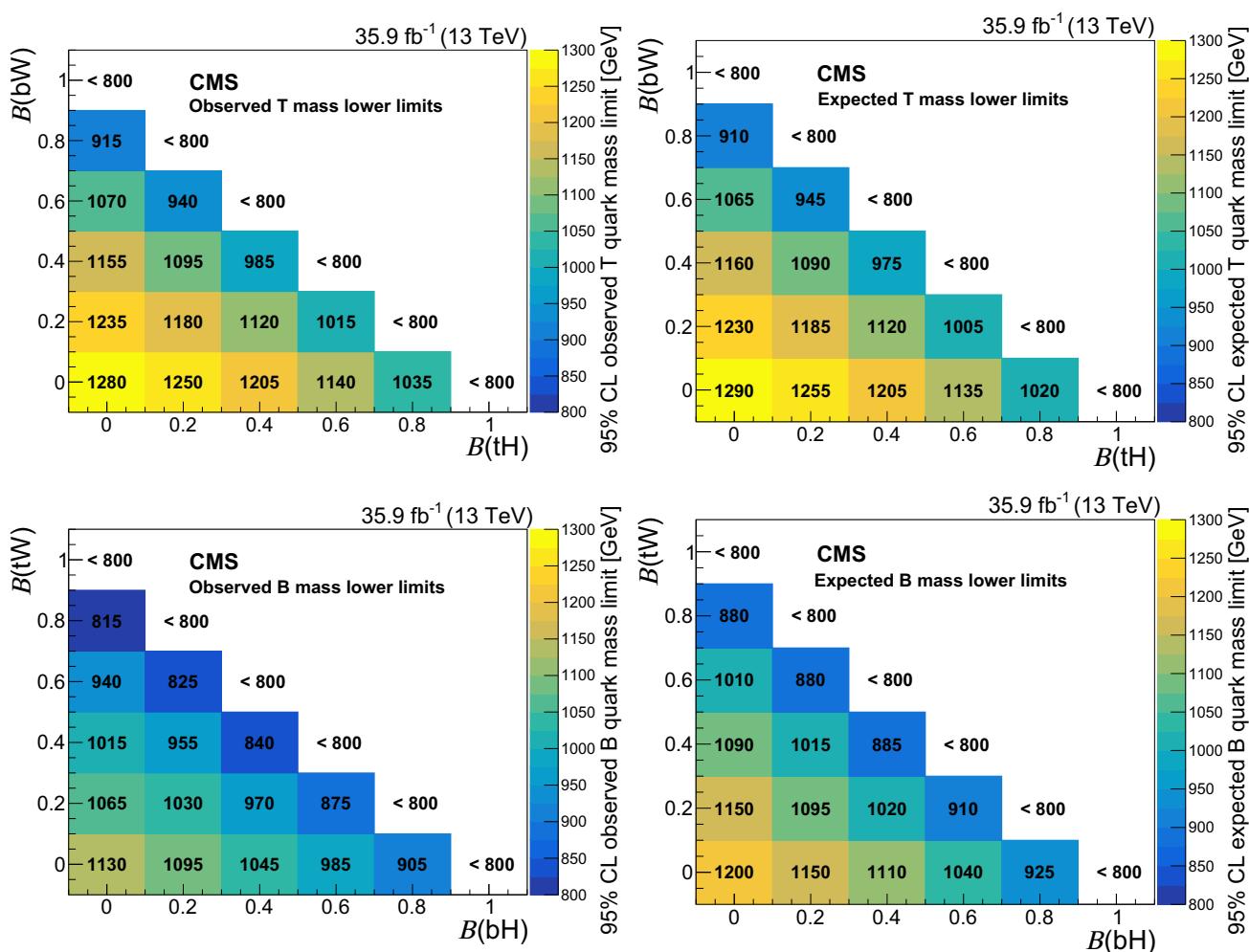
Fig. 5 The observed (left) and expected (right) 95% CL lower limits on the mass of the T (upper) and B (lower) quark, in GeV, for various branching fraction scenarios, assuming $\mathcal{B}(T \to tZ) + \mathcal{B}(T \to tH) + \mathcal{B}(T \to bW) = 1$ and $\mathcal{B}(B \to bZ) + \mathcal{B}(B \to bH) + \mathcal{B}(B \to tW) = 1$, respectively

$\mathcal{B}(B \to bH) + \mathcal{B}(B \to tW) = 1.0$. For a B quark decaying exclusively via $B \to bZ$, the lower mass limit is 1130 GeV.

8 Summary

The results of a search have been presented for the pair production of vector-like top (T) and bottom (B) quark partners in proton–proton collisions at $\sqrt{s} = 13$ TeV, using data collected by the CMS experiment at the CERN LHC, corresponding to an integrated luminosity of 35.9 fb^{-1}. The T$\overline{\text{T}}$ search is performed by looking for events in which one T quark decays via T $\to$ tZ and the other decays via T $\to$ bW, tZ, tH, where H refers to the Higgs boson. The B$\overline{\text{B}}$ search looks for events in which one B quark decays via B $\to$ bZ and the other via B $\to$ tW, bZ, or bH. Events with two oppositely charged electrons or muons, consistent with coming from the decay of a Z boson, and jets are investigated,

and are categorized according to the numbers of top quark and W, Z, and Higgs boson candidates. These categories are individually optimized for T$\overline{\text{T}}$ and B$\overline{\text{B}}$ event topologies.

The data are in agreement with the standard model background predictions for all the event categories. Upper limits at 95% confidence level on the T$\overline{\text{T}}$ and B$\overline{\text{B}}$ production cross sections are obtained from a simultaneous binned maximum-likelihood fit to the observed distributions for the different event categories, under the assumption of various T and B quark branching fractions. Comparing these upper limits to the theoretical predictions for the T$\overline{\text{T}}$ and B$\overline{\text{B}}$ cross sections as a function of the T and B quark masses, lower limits on the masses at 95% confidence level are determined for different branching fraction scenarios. In the case of a T quark decaying exclusively via T $\to$ tZ, the lower mass limit is 1280 GeV, while for a B quark decaying only via B $\to$ bZ, it is 1130 GeV. These lower limits are comparable with those measured by the ATLAS Collaboration [20], also using the

Table 8 The numbers of observed events and the predicted number of SM background events in the $B\overline{B}$ search for the five event categories using $Z \to e^+e^-$ channel. The expected numbers of signal events for B masses of 800 and 1200 GeV with branching fraction hypotheses for the three decay channels, $\mathcal{B}(B \to bZ) = 100\%$ (bZbZ), $\mathcal{B}(B \to bZ) =$ $\mathcal{B}(B \to bH) = 50\%$ (bZbH), and $\mathcal{B}(B \to bZ) = \mathcal{B}(B \to tW) = 50\%$ (bZtW) are also shown. The uncertainties in the number of expected background events include the statistical and systematic uncertainties added in quadrature

Event category		1b	2b	Boosted t	Boosted H	Boosted V
DY+jets		155.2 ± 10.4	23.5 ± 3.2	9.5 ± 1.8	1.9 ± 1.0	37.8 ± 4.4
$t\bar{t}$+jets		16.7 ± 3.1	6.9 ± 2.1	0.5 ± 0.6	0.3 ± 0.6	5.1 ± 1.8
$t\bar{t}Z$		6.0 ± 0.7	3.4 ± 0.5	3.3 ± 0.5	0.0 ± 0.4	5.2 ± 0.6
Other backgrounds		6.7 ± 3.8	1.3 ± 1.3	0.9 ± 0.6	0.0 ± 0.4	3.6 ± 2.5
Total		184.6 ± 12.7	35.1 ± 4.2	14.2 ± 2.1	2.5 ± 1.1	51.7 ± 5.3
Data		192	37	19	6	54
bZbZ,	$m_B = 800$ GeV	39.3 ± 1.8	24.6 ± 1.4	7.3 ± 0.8	2.1 ± 0.4	58.2 ± 2.3
bZbH,	$m_B = 800$ GeV	20.5 ± 0.7	18.2 ± 0.6	4.7 ± 0.3	4.6 ± 0.3	23.3 ± 0.7
bZtW,	$m_B = 800$ GeV	18.8 ± 0.6	11.5 ± 0.5	7.1 ± 0.4	1.0 ± 0.2	29.9 ± 0.8
bZbZ,	$m_B = 1200$ GeV	2.6 ± 0.1	1.3 ± 0.1	0.6 ± 0.1	0.2 ± 0.1	3.9 ± 0.2
bZbH,	$m_B = 1200$ GeV	1.4 ± 0.1	1.1 ± 0.1	0.4 ± 0.1	0.4 ± 0.1	1.6 ± 0.1
bZtW,	$m_B = 1200$ GeV	1.2 ± 0.1	0.6 ± 0.1	0.7 ± 0.1	0.1 ± 0.1	1.9 ± 0.1

Table 9 The number of observed events and the predicted number of SM background events in the $B\overline{B}$ search for the five event categories using $Z \to \mu^+\mu^-$ channel. The expected numbers of signal events for B masses of 800 and 1200 GeV with branching fraction hypotheses for the three decay channels, $\mathcal{B}(B \to bZ) = 100\%$ (bZbZ), $\mathcal{B}(B \to bZ) =$ $\mathcal{B}(B \to bH) = 50\%$ (bZbH), and $\mathcal{B}(B \to bZ) = \mathcal{B}(B \to tW) = 50\%$ (bZtW) are also shown. The uncertainties in the number of expected background events include the statistical and systematic uncertainties added in quadrature

| Event category		1b	2b	Boosted t	Boosted H	Boosted V
DY+jets		280.6 ± 20.2	38.1 ± 4.6	19.8 ± 3.2	5.0 ± 1.6	71.5 ± 7.6
$t\bar{t}$+jets		45.1 ± 5.6	20.0 ± 3.4	3.9 ± 1.3	0.6 ± 0.8	10.8 ± 2.9
$t\bar{t}Z$		9.0 ± 0.9	5.3 ± 0.6	5.4 ± 0.6	0.4 ± 0.4	8.0 ± 0.8
Other backgrounds		6.1 ± 4.2	1.2 ± 0.6	0.9 ± 0.5	0.1 ± 0.4	4.5 ± 3.1
Total		340.7 ± 22.3	64.5 ± 6.4	30.0 ± 3.7	6.1 ± 1.8	94.7 ± 9.1
Data		374	70	27	8	92
bZbZ,	$m_B = 800$ GeV	56.7 ± 2.1	38.8 ± 1.8	8.7 ± 0.9	2.3 ± 0.4	73.3 ± 2.6
bZbH,	$m_B = 800$ GeV	27.9 ± 0.8	27.5 ± 0.8	6.8 ± 0.4	6.7 ± 0.4	30.2 ± 0.8
bZtW,	$m_B = 800$ GeV	26.3 ± 0.7	16.2 ± 0.6	9.4 ± 0.5	1.2 ± 0.2	38.6 ± 0.9
bZbZ,	$m_B = 1200$ GeV	3.3 ± 0.1	1.9 ± 0.1	0.7 ± 0.1	0.1 ± 0.1	4.8 ± 0.2
bZbH,	$m_B = 1200$ GeV	1.7 ± 0.1	1.3 ± 0.1	0.5 ± 0.1	0.5 ± 0.1	2.0 ± 0.1
bZtW,	$m_B = 1200$ GeV	1.5 ± 0.1	0.8 ± 0.1	0.8 ± 0.1	0.1 ± 0.1	2.4 ± 0.1
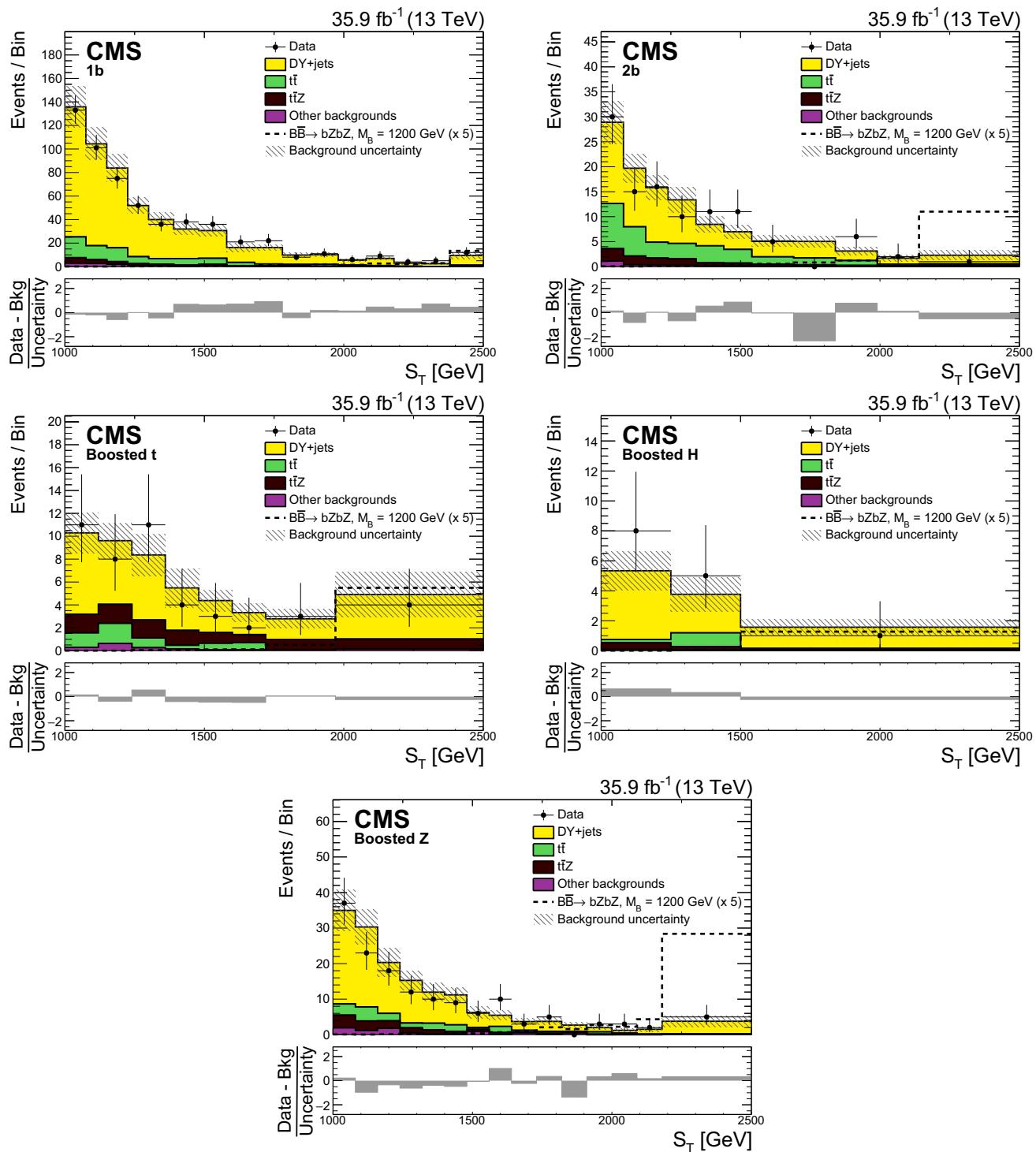
Fig. 6 The S_T distributions for the 1b, 2b, boosted t, boosted H and boosted Z (left to right, upper to lower) event categories for the data (points with vertical and horizontal bars), and the expected background (shaded histograms). The vertical bars give the statistical uncertainty in the data, and the horizontal bars show the bin widths. The expected signal for $B\overline{B} \rightarrow bZbZ$ with $m_B = 1200$ GeV multiplied by a factor of 5 is shown by the dashed line. The statistical and systematic uncertainties in the SM background prediction, added in quadrature, are represented by the hatched bands. The lower panel in each plot show the difference between the data and the expected background, divided by the total uncertainty
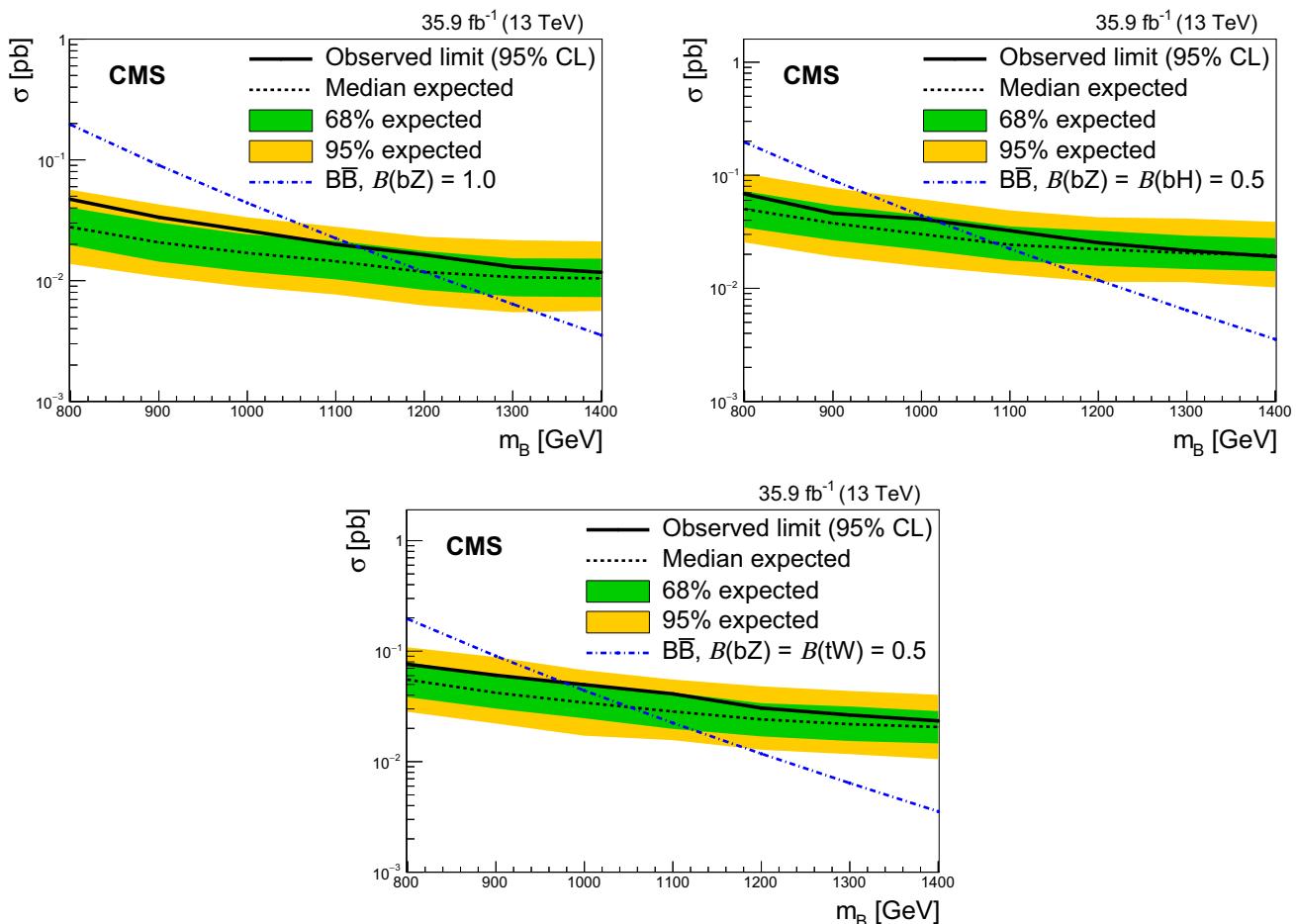
Fig. 7 The observed (solid line) and expected (dashed line) 95% CL upper limits on the $B\overline{B}$ production cross section versus the B quark mass for (upper left) $\mathcal{B}(B \to bZ) = 100\%$, (upper right) $\mathcal{B}(B \to bZ) = \mathcal{B}(B \to bH) = 50\%$, and (lower) $\mathcal{B}(B \to bZ) = \mathcal{B}(B \to tW) = 50\%$. The dotted-dashed line displays the theoretical cross section. The inner and outer bands show the one and two standard deviation uncertainties in the expected limits, respectively

Z boson dilepton decay channel. The results of the analysis presented in this paper are complementary to previous CMS measurements [21–23], and have extended sensitivity in reaching higher mass limits for T and B quarks.

References

1. ATLAS Collaboration, Observation of a new particle in the search for the Standard Model Higgs boson with the ATLAS detector at the LHC. Phys. Lett. B **716**, 1 (2012). https://doi.org/10.1016/j.physletb.2012.08.020. arXiv:1207.7214
2. CMS Collaboration, Observation of a new boson at a mass of 125 GeV with the CMS experiment at the LHC. Phys. Lett. B **716**, 30 (2012). https://doi.org/10.1016/j.physletb.2012.08.021. arXiv:1207.7235
3. CMS Collaboration, Observation of a new boson with mass near 125 GeV in pp collisions at $\sqrt{s} = 7$ and 8 TeV. JHEP **06**, 081 (2013). https://doi.org/10.1007/JHEP06(2013)081. arXiv:1303.4571
4. ATLAS and CMS Collaborations, Combined measurement of the Higgs boson mass in pp collisions at $\sqrt{s} = 7$ and 8 TeV with the ATLAS and CMS Experiments. Phys. Rev. Lett. **114**, 191803 (2015). https://doi.org/10.1103/PhysRevLett.114.191803. arXiv:1503.07589
5. CMS Collaboration, Measurements of properties of the Higgs boson decaying into the four-lepton final state in pp collisions at $\sqrt{s} = 13$ TeV. JHEP **11**, 047 (2017). https://doi.org/10.1007/JHEP11(2017)047. arXiv:1706.09936
6. J.A. Aguilar-Saavedra, R. Benbrik, S. Heinemeyer, M. Pérez-Victoria, Handbook of vectorlike quarks: mixing and single production. Phys. Rev. D **88**, 094010 (2013). https://doi.org/10.1103/PhysRevD.88.094010. arXiv:1306.0572
7. J. Kang, P. Langacker, B.D. Nelson, Theory and phenomenology of exotic isosinglet quarks and squarks. Phys. Rev. D **77**, 035003 (2008). https://doi.org/10.1103/PhysRevD.77.035003. arXiv:0708.2701v2
8. D. Choudhury, T. Tait, C. Wagner, Beautiful mirrors and precision electroweak data. Phys. Rev. D **65**, 053002 (2002). https://doi.org/10.1103/PhysRevD.65.053002. arXiv:hep-ph/0109097
9. L. Randall, R. Sundrum, A large mass hierarchy from a small extra dimension. Phys. Rev. Lett. **83**, 3370 (1999). https://doi.org/10.1103/PhysRevLett.83.3370. arXiv:hep-ph/9905221
10. N. Arkani-Hamed, A.G. Cohen, E. Katz, A.E. Nelson, The littlest Higgs. JHEP **07**, 034 (2002). https://doi.org/10.1088/1126-6708/2002/07/034. arXiv:hep-ph/0206021
11. M. Schmaltz, Physics beyond the standard model (theory): introducing the Little Higgs. Nucl. Phys. Proc. Suppl. **117**, 40 (2003). https://doi.org/10.1016/S0920-5632(03)01409-9. arXiv:hep-ph/0210415
12. M. Schmaltz, D. Tucker-Smith, Little Higgs review. Ann. Rev. Nucl. Part. Sci. **55**, 229 (2005). https://doi.org/10.1146/annurev.nucl.55.090704.151502. arXiv:hep-ph/0502182
13. M.S.D. Marzocca, J. Shu, General composite Higgs models. JHEP **08**, 013 (2012). https://doi.org/10.1007/JHEP08(2012)013. arXiv:1205.0770
14. D. Guadagnoli, R.N. Mohapatra, I. Sung, Gauged flavor group with left-right symmetry. JHEP **04**, 093 (2011). https://doi.org/10.1007/JHEP04(2011)093. arXiv:1103.4170
15. R.T. D'Agnolo, A. Hook, Finding the strong CP problem at the LHC. Phys. Lett. B **762**, 421 (2016). https://doi.org/10.1016/j.physletb.2016.09.061. arXiv:1507.00336
16. Y. Okada, L. Panizzi, LHC signatures of vector-like quarks. Adv. High Energy Phys. **2013**, 364936 (2013). https://doi.org/10.1155/2013/364936. arXiv:1207.5607
17. ATLAS Collaboration, Search for pair production of vector-like top quarks in events with one lepton, jets, and missing transverse momentum in $\sqrt{s} = 13$ TeV pp collisions with the atlas detector. *JHEP* **08**, 052 (2017) https://doi.org/10.1007/JHEP08(2017)052. arXiv:1705.10751
18. ATLAS Collaboration, Search for pair production of heavy vector-like quarks decaying to high-p_T W bosons and b quarks in the lepton-plus-jets final state in pp collisions at $\sqrt{s} = 13$ TeV with the atlas detector. JHEP **10**, 141(2017). https://doi.org/10.1007/JHEP10(2017)141. arXiv:1707.03347
19. ATLAS Collaboration, Search for pair production of vector-like quarks into high-p_T W bosons and top quarks in the lepton-plus-jets final state in pp collisions at $\sqrt{s} = 13$ TeV with the ATLAS detector. JHEP **08**, 48 (2018). https://doi.org/10.1007/JHEP08(2018)048. arXiv:1806.01762
20. ATLAS Collaboration, Search for pair and single production of vectorlike quarks in final states with at least one Z boson decaying into a pair of electrons or muons in pp collision data collected with the ATLAS detector at $\sqrt{s} = 13$ TeV. Phys. Rev. D **98**, 112010 (2018). https://doi.org/10.1103/PhysRevD.98.112010. arXiv:1806.10555
21. CMS Collaboration, Search for pair production of vector-like T and B quarks in single-lepton final states using boosted jet substructure in proton–proton collisions at $\sqrt{s} = 13$ TeV. JHEP **11**, 085 (2017). https://doi.org/10.1007/JHEP11(2017)085. arXiv:1706.03408
22. CMS Collaboration, Search for pair production of vector-like quarks in the bW$\bar{b}$W channel from proton–proton collisions at $\sqrt{s} = 13$ TeV. Phys. Lett. B **779**, 82 (2018). https://doi.org/10.1016/j.physletb.2018.01.077. arXiv:1710.01539
23. CMS Collaboration, Search for vector-like T and B quark pairs in final states with leptons at $\sqrt{s} = 13$ TeV. JHEP **08**, 177 (2018). https://doi.org/10.1007/JHEP08(2018)177. arXiv:1805.04758
24. CMS Collaboration, The CMS experiment at the CERN LHC. JINST **3**, S08004 (2008). https://doi.org/10.1088/1748-0221/3/08/S08004
25. CMS Collaboration, The CMS trigger system. JINST **12**, P01020 (2017). https://doi.org/10.1088/1748-0221/12/01/P01020. arXiv:1609.02366

26. J. Alwall et al., The automated computation of tree-level and next-to-leading order differential cross sections, and their matching to parton shower simulations. JHEP **07**, 079 (2014). https://doi.org/10.1007/JHEP07(2014)079. arXiv:1405.0301

27. NNPDF Collaboration, Parton distributions for the LHC Run II. JHEP **04**, 040 (2015) https://doi.org/10.1007/JHEP04(2015)040. arXiv:1410.8849

28. T. Sjöstrand et al., An introduction to PYTHIA 8.2. Comput. Phys. Commun. **191**, 159 (2015). https://doi.org/10.1016/j.cpc.2015.01.024. arXiv:1410.3012

29. CMS Collaboration, Event generator tunes obtained from underlying event and multiparton scattering measurements. Eur. Phys. J. C **76**, 155 (2016). https://doi.org/10.1140/epjc/s10052-016-3988-x. arXiv:1512.00815

30. M. Czakon, P. Fiedler, A. Mitov, Total top quark pair production cross section at hadron colliders through $O(\alpha_S^4)$. Phys. Rev. Lett. **110**, 252004 (2013). https://doi.org/10.1103/PhysRevLett.110.252004. arXiv:1303.6254

31. M.R. Whalley, D. Bourilkov, R.C. Group, The Les Houches accord PDFs (LHAPDF) and LHAGLUE (2005). arXiv:hep-ph/0508110

32. S. Frixione, B.R. Webber, Matching NLO QCD computations and parton shower simulations. JHEP **06**, 029 (2002). https://doi.org/10.1088/1126-6708/2002/06/029. arXiv:hep-ph/0204244

33. R. Frederix, S. Frixione, Merging meets matching in MC@NLO. JHEP **12**, 061 (2012). https://doi.org/10.1007/JHEP12(2012)061. arXiv:1209.6215

34. S. Frixione, G. Ridolfi, P. Nason, A positive-weight next-to-leading-order Monte Carlo for heavy flavour hadroproduction. JHEP **09**, 126 (2007). https://doi.org/10.1088/1126-6708/2007/09/126. arXiv:0707.3088

35. S. Frixione, P. Nason, C. Oleari, Matching NLO QCD computations with parton shower simulations: the POWHEG method. JHEP **11**, 070 (2007). https://doi.org/10.1088/1126-6708/2007/11/070. arXiv:0709.2092

36. S. Alioli, P. Nason, C. Oleari, E. Re, A general framework for implementing NLO calculations in shower Monte Carlo programs: the POWHEG BOX. JHEP **06**, 043 (2010). https://doi.org/10.1007/JHEP06(2010)043. arXiv:1002.2581

37. CMS Collaboration, Investigations of the impact of the parton shower tuning in PYTHIA 8 in the modelling of $t\bar{t}$ at $\sqrt{s} = 8$ and 13 TeV. CMS Detector Performance Summary CMS-PAS-TOP-16-021, CERN (2016)

38. J. Alwall et al., Comparative study of various algorithms for the merging of parton showers and matrix elements in hadronic collisions. Eur. Phys. J. C **53**, 473 (2008). https://doi.org/10.1140/epjc/s10052-007-0490-5. arXiv:0706.2569

39. J.M. Campbell, R.K. Ellis, C. Williams, Vector boson pair production at the LHC. JHEP **07**, 018 (2011). https://doi.org/10.1007/JHEP07(2011)018. arXiv:1105.0020

40. F. Cascioli et al., ZZ production at hadron colliders in NNLO QCD. Phys. Lett. B **735**, 311 (2014). https://doi.org/10.1016/j.physletb.2014.06.056. arXiv:1405.2219v2

41. T. Gehrmann et al., W^+W^- production at hadron colliders in NNLO QCD. Phys. Rev. Lett. **113**, 212001 (2014). https://doi.org/10.1103/PhysRevLett.113.212001. arXiv:1408.5243

42. D. de Florian et al., Handbook of LHC Higgs cross sections: 4. Deciphering the nature of the Higgs sector. CERN Report CERN-2017-002-M, CERN (2016). https://doi.org/10.23731/CYRM-2017-002. arXiv:1610.07922

43. GEANT4 Collaboration, GEANT4—a simulation toolkit. Nucl. Instrum. Methods A **506**, 250 (2003). https://doi.org/10.1016/S0168-9002(03)01368-8

44. J. Allison et al., GEANT4 developments and applications. IEEE Trans. Nucl. Sci. **53**, 270 (2006). https://doi.org/10.1109/TNS.2006.869826

45. CMS Collaboration, Particle-flow reconstruction and global event description with the CMS detector. JINST **12**, P10003 (2017). https://doi.org/10.1088/1748-0221/12/10/P10003. arXiv:1706.04965

46. CMS Collaboration, Description and performance of track and primary-vertex reconstruction with the CMS tracker. JINST **9**, P10009 (2014). https://doi.org/10.1088/1748-0221/9/10/P10009. arXiv:1405.6569

47. M. Cacciari, G.P. Salam, G. Soyez, The anti-k_T jet clustering algorithm. JHEP **04**, 063 (2008). https://doi.org/10.1088/1126-6708/2008/04/063. arXiv:0802.1189

48. M. Cacciari, G.P. Salam, G. Soyez, FastJet user manual. Eur. Phys. J. C **72**, 1896 (2012). https://doi.org/10.1140/epjc/s10052-012-1896-2. arXiv:1111.6097

49. CMS Collaboration, Performance of electron reconstruction and selection with the CMS detector in proton–proton collisions at $\sqrt{s} = 8$ TeV. JINST **10**, P06005 (2015). https://doi.org/10.1088/1748-0221/10/06/P06005. arXiv:1502.02701

50. CMS Collaboration, Commissioning of the particle-flow event reconstruction with the first LHC collisions recorded in the CMS detector. CMS Physics Analysis Summary CMS-PAS-PFT-10-001, CERN (2010)

51. CMS Collaboration, Performance of the CMS muon detector and muon reconstruction with proton–proton collisions at $\sqrt{s} = 13$ TeV. JINST **13**, P06015 (2018). https://doi.org/10.1088/1748-0221/13/06/P06015. arXiv:1804.04528

52. M. Cacciari, G.P. Salam, Pileup subtraction using jet areas. Phys. Lett. B **659**, 119 (2008). https://doi.org/10.1016/j.physletb.2007.09.077. arXiv:0707.1378

53. CMS Collaboration, Determination of jet energy calibration and transverse momentum resolution in CMS. JINST **6**, P11002 (2011). https://doi.org/10.1088/1748-0221/6/11/P11002. arXiv:1107.4277

54. CMS Collaboration, Jet energy scale and resolution in the CMS experiment in pp collisions at 8 TeV. JINST **12**, P02014 (2017). https://doi.org/10.1088/1748-0221/12/02/P02014. arXiv:1607.03663

55. CMS Collaboration, Identification of heavy-flavour jets with the CMS detector in pp collisions at 13 TeV. JINST **13**, P05011 (2018). https://doi.org/10.1088/1748-0221/13/05/P05011. arXiv:1712.07158

56. CMS Collaboration, Performance of CMS muon reconstruction in pp collision events at $\sqrt{s} = 7$ TeV. JINST **7**, P10002 (2012). https://doi.org/10.1088/1748-0221/7/10/P10002. arXiv:1206.4071

57. S.D. Ellis, C.K. Vermilion, J.R. Walsh, Techniques for improved heavy particle searches with jet substructure. Phys. Rev. D **80**, 051501 (2009). https://doi.org/10.1103/PhysRevD.80.051501. arXiv:0903.5081

58. S.D. Ellis, C.K. Vermilion, J.R. Walsh, Recombination algorithms and jet substructure: pruning as a tool for heavy particle searches. Phys. Rev. D **81**, 094023 (2010). https://doi.org/10.1103/PhysRevD.81.094023. arXiv:0912.0033

59. G.P. Salam, Towards jetography. Eur. Phys. J. C **67**, 637 (2010). https://doi.org/10.1140/epjc/s10052-010-1314-6. arXiv:0906.1833

60. J. Thaler, K. Van Tilburg, Identifying boosted objects with N-subjettiness. JHEP **03**, 015 (2011). https://doi.org/10.1007/JHEP03(2011)015. arXiv:1011.2268

61. M. Dasgupta, A. Fregoso, S. Marzani, G.P. Salam, Towards an understanding of jet substructure. JHEP **09**, 029 (2013). https://doi.org/10.1007/JHEP09(2013)029. arXiv:1307.0007

62. A.J. Larkoski, S. Marzani, G. Soyez, J. Thaler, Soft drop. JHEP **05**, 146 (2014). https://doi.org/10.1007/JHEP05(2014)146. arXiv:1402.2657

63. CMS Collaboration, Jet algorithms performance in 13 TeV data. CMS Physics Analysis Summary CMS-PAS-JME-16-003, CERN (2017)

64. CMS Collaboration, Search for a massive resonance decaying to a pair of Higgs bosons in the four b quark final state in proton–proton collisions at $\sqrt{s} = 13$ TeV. Phys. Lett. B **781**, 244 (2018). https://doi.org/10.1016/j.physletb.2018.03.084. arXiv:1710.04960

65. M. Bahr et al., Herwig++ physics and manual. Eur. Phys. J. C **58**, 639 (2008). https://doi.org/10.1140/epjc/s10052-008-0798-9. arXiv:0803.0883

66. CMS Collaboration, Measurement of differential cross sections for Z boson production in association with jets in proton–proton collisions at $\sqrt{s} = 13$ TeV. Eur. Phys. J. C **78**, 965 (2018). https://doi.org/10.1140/epjc/s10052-018-6373-0. arXiv:1804.05252

67. CMS Collaboration, Measurement of differential cross sections for top quark pair production using the lepton+jets final state in proton–proton collisions at 13 TeV. Phys. Rev. D **95**, 092001 (2017). https://doi.org/10.1103/PhysRevD.95.092001. arXiv:1610.04191

68. CMS Collaboration, Measurements of the pp → ZZ production cross section and the Z → 4ℓ branching fraction, and constraints on anomalous triple gauge couplings at $\sqrt{s} = 13$ TeV. Eur. Phys. J. C **78**, 165 (2018). https://doi.org/10.1140/epjc/s10052-018-5567-9. arXiv:1709.08601

69. CMS Collaboration, CMS luminosity measurement for the 2016 data taking period. CMS Physics Analysis Summary CMS-PAS-LUM-17-001, CERN (2017)

70. J. Butterworth et al., PDF4LHC recommendations for LHC Run II. J. Phys. G **43**, 023001 (2016). https://doi.org/10.1088/0954-3899/43/2/023001. arXiv:1510.03865

71. S. Dulat et al., The CT14 global analysis of quantum chromodynamics. Phys. Rev. D **93**, 033006 (2015). https://doi.org/10.1103/PhysRevD.93.033006. arXiv:1506.07443

72. L.A. Harland-Lang, A.D. Martin, P. Motylinski, R.S. Thorne, Parton distributions in the LHC era: MMHT 2014 PDFs. Eur. Phys. J. C **75**, 204 (2015). https://doi.org/10.1140/epjc/s10052-015-3397-6. arXiv:1412.3989

73. CMS Collaboration, Jet energy scale and resolution performances with 13 TeV data. CMS Detector Performance Summary CMS-DP-2016-020, CERN (2016)

74. Particle Data Group, M. Tanabashi et al., Review of particle physics. Phys. Rev. D **98**, 030001 (2018). https://doi.org/10.1103/PhysRevD.98.030001

75. J. Ott, THETA—a framework for template-based modeling and inference (2010). http://www-ekp.physik.uni-karlsruhe.de/~ott/theta/theta-auto. Accessed 30 Oct 2014

CMS Collaboration

Yerevan Physics Institute, Yerevan, Armenia
A. M. Sirunyan, A. Tumasyan

Institut für Hochenergiephysik, Vienna, Austria
W. Adam, F. Ambrogi, E. Asilar, T. Bergauer, J. Brandstetter, M. Dragicevic, J. Erö, A. Escalante Del Valle, M. Flechl, R. Frühwirth[1], V. M. Ghete, J. Hrubec, M. Jeitler[1], N. Krammer, I. Krätschmer, D. Liko, T. Madlener, I. Mikulec, N. Rad, H. Rohringer, J. Schieck[1], R. Schöfbeck, M. Spanring, D. Spitzbart, W. Waltenberger, J. Wittmann, C.-E. Wulz[1], M. Zarucki

Institute for Nuclear Problems, Minsk, Belarus
V. Chekhovsky, V. Mossolov, J. Suarez Gonzalez

Universiteit Antwerpen, Antwerp, Belgium
E. A. De Wolf, D. Di Croce, X. Janssen, J. Lauwers, M. Pieters, H. Van Haevermaet, P. Van Mechelen, N. Van Remortel

Vrije Universiteit Brussel, Brussels, Belgium
S. Abu Zeid, F. Blekman, J. D'Hondt, J. De Clercq, K. Deroover, G. Flouris, D. Lontkovskyi, S. Lowette, I. Marchesini, S. Moortgat, L. Moreels, Q. Python, K. Skovpen, S. Tavernier, W. Van Doninck, P. Van Mulders, I. Van Parijs

Université Libre de Bruxelles, Brussels, Belgium
D. Beghin, B. Bilin, H. Brun, B. Clerbaux, G. De Lentdecker, H. Delannoy, B. Dorney, G. Fasanella, L. Favart, R. Goldouzian, A. Grebenyuk, A. K. Kalsi, T. Lenzi, J. Luetic, N. Postiau, E. Starling, L. Thomas, C. Vander Velde, P. Vanlaer, D. Vannerom, Q. Wang

Ghent University, Ghent, Belgium
T. Cornelis, D. Dobur, A. Fagot, M. Gul, I. Khvastunov[2], D. Poyraz, C. Roskas, D. Trocino, M. Tytgat, W. Verbeke, B. Vermassen, M. Vit, N. Zaganidis

Université Catholique de Louvain, Louvain-la-Neuve, Belgium
H. Bakhshiansohi, O. Bondu, S. Brochet, G. Bruno, C. Caputo, P. David, C. Delaere, M. Delcourt, A. Giammanco, G. Krintiras, V. Lemaitre, A. Magitteri, K. Piotrzkowski, A. Saggio, M. Vidal Marono, P. Vischia, S. Wertz, J. Zobec

Centro Brasileiro de Pesquisas Fisicas, Rio de Janeiro, Brazil
F. L. Alves, G. A. Alves, M. Correa Martins Junior, G. Correia Silva, C. Hensel, A. Moraes, M. E. Pol, P. Rebello Teles

Universidade do Estado do Rio de Janeiro, Rio de Janeiro, Brazil

E. Belchior Batista Das Chagas, W. Carvalho, J. Chinellato[3], E. Coelho, E. M. Da Costa, G. G. Da Silveira[4], D. De Jesus Damiao, C. De Oliveira Martins, S. Fonseca De Souza, H. Malbouisson, D. Matos Figueiredo, M. Melo De Almeida, C. Mora Herrera, L. Mundim, H. Nogima, W. L. Prado Da Silva, L. J. Sanchez Rosas, A. Santoro, A. Sznajder, M. Thiel, E. J. Tonelli Manganote[3], F. Torres Da Silva De Araujo, A. Vilela Pereira

Universidade Estadual Paulista[a], Universidade Federal do ABC[b], São Paulo, Brazil

S. Ahuja[a], C. A. Bernardes[a], L. Calligaris[a], T. R. Fernandez Perez Tomei[a], E. M. Gregores[b], P. G. Mercadante[b], S. F. Novaes[a], Sandra S. Padula[a]

Institute for Nuclear Research and Nuclear Energy, Bulgarian Academy of Sciences, Sofia, Bulgaria

A. Aleksandrov, R. Hadjiiska, P. Iaydjiev, A. Marinov, M. Misheva, M. Rodozov, M. Shopova, G. Sultanov

University of Sofia, Sofia, Bulgaria

A. Dimitrov, L. Litov, B. Pavlov, P. Petkov

Beihang University, Beijing, China

W. Fang[5], X. Gao[5], L. Yuan

Institute of High Energy Physics, Beijing, China

M. Ahmad, J. G. Bian, G. M. Chen, H. S. Chen, M. Chen, Y. Chen, C. H. Jiang, D. Leggat, H. Liao, Z. Liu, S. M. Shaheen[6], A. Spiezia, J. Tao, Z. Wang, E. Yazgan, H. Zhang, S. Zhang[6], J. Zhao

State Key Laboratory of Nuclear Physics and Technology, Peking University, Beijing, China

Y. Ban, G. Chen, A. Levin, J. Li, L. Li, Q. Li, Y. Mao, S. J. Qian, D. Wang

Tsinghua University, Beijing, China

Y. Wang

Universidad de Los Andes, Bogotá, Colombia

C. Avila, A. Cabrera, C. A. Carrillo Montoya, L. F. Chaparro Sierra, C. Florez, C. F. González Hernández, M. A. Segura Delgado

Faculty of Electrical Engineering, Mechanical Engineering and Naval Architecture, University of Split, Split, Croatia

B. Courbon, N. Godinovic, D. Lelas, I. Puljak, T. Sculac

Faculty of Science, University of Split, Split, Croatia

Z. Antunovic, M. Kovac

Institute Rudjer Boskovic, Zagreb, Croatia

V. Brigljevic, D. Ferencek, K. Kadija, B. Mesic, M. Roguljic, A. Starodumov[7], T. Susa

University of Cyprus, Nicosia, Cyprus

M. W. Ather, A. Attikis, M. Kolosova, G. Mavromanolakis, J. Mousa, C. Nicolaou, F. Ptochos, P. A. Razis, H. Rykaczewski

Charles University, Prague, Czech Republic

M. Finger[8], M. Finger Jr.[8]

Escuela Politecnica Nacional, Quito, Ecuador

E. Ayala

Universidad San Francisco de Quito, Quito, Ecuador

E. Carrera Jarrin

Academy of Scientific Research and Technology of the Arab Republic of Egypt, Egyptian Network of High Energy Physics, Cairo, Egypt

A. Mahrous[9], A. Mohamed[10], Y Mohammed[11]

National Institute of Chemical Physics and Biophysics, Tallinn, Estonia

S. Bhowmik, A. Carvalho Antunes De Oliveira, R. K. Dewanjee, K. Ehataht, M. Kadastik, M. Raidal, C. Veelken

Department of Physics, University of Helsinki, Helsinki, Finland
P. Eerola, H. Kirschenmann, J. Pekkanen, M. Voutilainen

Helsinki Institute of Physics, Helsinki, Finland
J. Havukainen, J. K. Heikkilä, T. Järvinen, V. Karimäki, R. Kinnunen, T. Lampén, K. Lassila-Perini, S. Laurila, S. Lehti,
T. Lindén, P. Luukka, T. Mäenpää, H. Siikonen, E. Tuominen, J. Tuominiemi

Lappeenranta University of Technology, Lappeenranta, Finland
T. Tuuva

IRFU, CEA, Université Paris-Saclay, Gif-sur-Yvette, France
M. Besancon, F. Couderc, M. Dejardin, D. Denegri, J. L. Faure, F. Ferri, S. Ganjour, A. Givernaud, P. Gras,
G. Hamel de Monchenault, P. Jarry, C. Leloup, E. Locci, J. Malcles, G. Negro, J. Rander, A. Rosowsky, M. Ö. Sahin,
M. Titov

Laboratoire Leprince-Ringuet, Ecole polytechnique, CNRS/IN2P3, Université Paris-Saclay, Palaiseau, France
A. Abdulsalam[12], C. Amendola, I. Antropov, F. Beaudette, P. Busson, C. Charlot, R. Granier de Cassagnac, I. Kucher,
A. Lobanov, J. Martin Blanco, C. Martin Perez, M. Nguyen, C. Ochando, G. Ortona, P. Paganini, J. Rembser, R. Salerno,
J. B. Sauvan, Y. Sirois, A. G. Stahl Leiton, A. Zabi, A. Zghiche

Université de Strasbourg, CNRS, IPHC UMR 7178, Strasbourg, France
J.-L. Agram[13], J. Andrea, D. Bloch, J.-M. Brom, E. C. Chabert, V. Cherepanov, C. Collard, E. Conte[13], J.-C. Fontaine[13],
D. Gelé, U. Goerlach, M. Jansová, A.-C. Le Bihan, N. Tonon, P. Van Hove

**Centre de Calcul de l'Institut National de Physique Nucleaire et de Physique des Particules, CNRS/IN2P3,
Villeurbanne, France**
S. Gadrat

**Université de Lyon, Université Claude Bernard Lyon 1, CNRS-IN2P3, Institut de Physique Nucléaire de Lyon,
Villeurbanne, France**
S. Beauceron, C. Bernet, G. Boudoul, N. Chanon, R. Chierici, D. Contardo, P. Depasse, H. El Mamouni, J. Fay, L. Finco,
S. Gascon, M. Gouzevitch, G. Grenier, B. Ille, F. Lagarde, I. B. Laktineh, H. Lattaud, M. Lethuillier, L. Mirabito,
S. Perries, A. Popov[14], V. Sordini, G. Touquet, M. Vander Donckt, S. Viret

Georgian Technical University, Tbilisi, Georgia
T. Toriashvili[15]

Tbilisi State University, Tbilisi, Georgia
Z. Tsamalaidze[8]

I. Physikalisches Institut, RWTH Aachen University, Aachen, Germany
C. Autermann, L. Feld, M. K. Kiesel, K. Klein, M. Lipinski, M. Preuten, M. P. Rauch, C. Schomakers, J. Schulz,
M. Teroerde, B. Wittmer

III. Physikalisches Institut A, RWTH Aachen University, Aachen, Germany
A. Albert, D. Duchardt, M. Erdmann, S. Erdweg, T. Esch, R. Fischer, S. Ghosh, A. Güth, T. Hebbeker, C. Heidemann,
K. Hoepfner, H. Keller, L. Mastrolorenzo, M. Merschmeyer, A. Meyer, P. Millet, S. Mukherjee, T. Pook, M. Radziej,
H. Reithler, M. Rieger, A. Schmidt, D. Teyssier, S. Thüer

III. Physikalisches Institut B, RWTH Aachen University, Aachen, Germany
G. Flügge, O. Hlushchenko, T. Kress, T. Müller, A. Nehrkorn, A. Nowack, C. Pistone, O. Pooth, D. Roy, H. Sert, A. Stahl[16]

Deutsches Elektronen-Synchrotron, Hamburg, Germany
M. Aldaya Martin, T. Arndt, C. Asawatangtrakuldee, I. Babounikau, K. Beernaert, O. Behnke, U. Behrens,
A. Bermúdez Martínez, D. Bertsche, A. A. Bin Anuar, K. Borras[17], V. Botta, A. Campbell, P. Connor,
C. Contreras-Campana, V. Danilov, A. De Wit, M. M. Defranchis, C. Diez Pardos, D. Domínguez Damiani, G. Eckerlin,
T. Eichhorn, A. Elwood, E. Eren, E. Gallo[18], A. Geiser, J. M. Grados Luyando, A. Grohsjean, M. Guthoff, M. Haranko,
A. Harb, H. Jung, M. Kasemann, J. Keaveney, C. Kleinwort, J. Knolle, D. Krücker, W. Lange, A. Lelek, T. Lenz,
J. Leonard, K. Lipka, W. Lohmann[19], R. Mankel, I.-A. Melzer-Pellmann, A. B. Meyer, M. Meyer, M. Missiroli, J. Mnich,

V. Myronenko, S. K. Pflitsch, D. Pitzl, A. Raspereza, P. Saxena, P. Schütze, C. Schwanenberger, R. Shevchenko, A. Singh, H. Tholen, O. Turkot, A. Vagnerini, M. Van De Klundert, G. P. Van Onsem, R. Walsh, Y. Wen, K. Wichmann, C. Wissing, O. Zenaiev

University of Hamburg, Hamburg, Germany
R. Aggleton, S. Bein, L. Benato, A. Benecke, V. Blobel, T. Dreyer, A. Ebrahimi, E. Garutti, D. Gonzalez, P. Gunnellini, J. Haller, A. Hinzmann, A. Karavdina, G. Kasieczka, R. Klanner, R. Kogler, N. Kovalchuk, S. Kurz, V. Kutzner, J. Lange, D. Marconi, J. Multhaup, M. Niedziela, C.E.N. Niemeyer, D. Nowatschin, A. Perieanu, A. Reimers, O. Rieger, C. Scharf, P. Schleper, S. Schumann, J. Schwandt, J. Sonneveld, H. Stadie, G. Steinbrück, F. M. Stober, M. Stöver, B. Vormwald, I. Zoi

Karlsruher Institut fuer Technologie, Karlsruhe, Germany
M. Akbiyik, C. Barth, M. Baselga, S. Baur, E. Butz, R. Caspart, T. Chwalek, F. Colombo, W. De Boer, A. Dierlamm, K. El Morabit, N. Faltermann, B. Freund, M. Giffels, M. A. Harrendorf, F. Hartmann[16], S. M. Heindl, U. Husemann, I. Katkov[14], S. Kudella, S. Mitra, M. U. Mozer, Th. Müller, M. Musich, M. Plagge, G. Quast, K. Rabbertz, M. Schröder, I. Shvetsov, H. J. Simonis, R. Ulrich, S. Wayand, M. Weber, T. Weiler, C. Wöhrmann, R. Wolf

Institute of Nuclear and Particle Physics (INPP), NCSR Demokritos, Aghia Paraskevi, Greece
G. Anagnostou, G. Daskalakis, T. Geralis, A. Kyriakis, D. Loukas, G. Paspalaki

National and Kapodistrian University of Athens, Athens, Greece
A. Agapitos, G. Karathanasis, P. Kontaxakis, A. Panagiotou, I. Papavergou, N. Saoulidou, E. Tziaferi, K. Vellidis

National Technical University of Athens, Athens, Greece
K. Kousouris, I. Papakrivopoulos, G. Tsipolitis

University of Ioánnina, Ioannina, Greece
I. Evangelou, C. Foudas, P. Gianneios, P. Katsoulis, P. Kokkas, S. Mallios, N. Manthos, I. Papadopoulos, E. Paradas, J. Strologas, F. A. Triantis, D. Tsitsonis

MTA-ELTE Lendület CMS Particle and Nuclear Physics Group, Eötvös Loránd University, Budapest, Hungary
M. Bartók[20], M. Csanad, N. Filipovic, P. Major, M. I. Nagy, G. Pasztor, O. Surányi, G. I. Veres

Wigner Research Centre for Physics, Budapest, Hungary
G. Bencze, C. Hajdu, D. Horvath[21], Á. Hunyadi, F. Sikler, T. Á. Vámi, V. Veszpremi, G. Vesztergombi[†]

Institute of Nuclear Research ATOMKI, Debrecen, Hungary
N. Beni, S. Czellar, J. Karancsi[20], A. Makovec, J. Molnar, Z. Szillasi

Institute of Physics, University of Debrecen, Debrecen, Hungary
P. Raics, Z. L. Trocsanyi, B. Ujvari

Indian Institute of Science (IISc), Bangalore, India
S. Choudhury, J. R. Komaragiri, P. C. Tiwari

National Institute of Science Education and Research, HBNI, Bhubaneswar, India
S. Bahinipati[23], C. Kar, P. Mal, K. Mandal, A. Nayak[24], S. Roy Chowdhury, D. K. Sahoo[23], S. K. Swain

Panjab University, Chandigarh, India
S. Bansal, S. B. Beri, V. Bhatnagar, S. Chauhan, R. Chawla, N. Dhingra, S. K. Gill, R. Gupta, A. Kaur, M. Kaur, P. Kumari, M. Lohan, M. Meena, A. Mehta, K. Sandeep, S. Sharma, J. B. Singh, A. K. Virdi, G. Walia

University of Delhi, Delhi, India
A. Bhardwaj, B. C. Choudhary, R. B. Garg, M. Gola, S. Keshri, Ashok Kumar, S. Malhotra, M. Naimuddin, P. Priyanka, K. Ranjan, Aashaq Shah, R. Sharma

Saha Institute of Nuclear Physics, HBNI, Kolkata, India
R. Bhardwaj[25], M. Bharti[25], R. Bhattacharya, S. Bhattacharya, U. Bhawandeep[25], D. Bhowmik, S. Dey, S. Dutt[25], S. Dutta, S. Ghosh, K. Mondal, S. Nandan, A. Purohit, P. K. Rout, A. Roy, G. Saha, S. Sarkar, M. Sharan, B. Singh[25], S. Thakur[25]

Indian Institute of Technology Madras, Madras, India
P. K. Behera, A. Muhammad

Bhabha Atomic Research Centre, Mumbai, India
R. Chudasama, D. Dutta, V. Jha, V. Kumar, D. K. Mishra, P. K. Netrakanti, L. M. Pant, P. Shukla, P. Suggisetti

Tata Institute of Fundamental Research-A, Mumbai, India
T. Aziz, M. A. Bhat, S. Dugad, G. B. Mohanty, N. Sur, RavindraKumar Verma

Tata Institute of Fundamental Research-B, Mumbai, India
S. Banerjee, S. Bhattacharya, S. Chatterjee, P. Das, M. Guchait, Sa. Jain, S. Karmakar, S. Kumar, M. Maity[26],
G. Majumder, K. Mazumdar, N. Sahoo, T. Sarkar[26]

Indian Institute of Science Education and Research (IISER), Pune, India
S. Chauhan, S. Dube, V. Hegde, A. Kapoor, K. Kothekar, S. Pandey, A. Rane, A. Rastogi, S. Sharma

Institute for Research in Fundamental Sciences (IPM), Tehran, Iran
S. Chenarani[27], E. Eskandari Tadavani, S. M. Etesami[27], M. Khakzad, M. Mohammadi Najafabadi, M. Naseri,
F. Rezaei Hosseinabadi, B. Safarzadeh[28], M. Zeinali

University College Dublin, Dublin, Ireland
M. Felcini, M. Grunewald

INFN Sezione di Bari[a], Università di Bari[b], Politecnico di Bari[c], Bari, Italy
M. Abbrescia[a,b], C. Calabria[a,b], A. Colaleo[a], D. Creanza[a,c], L. Cristella[a,b], N. De Filippis[a,c], M. De Palma[a,b],
A. Di Florio[a,b], F. Errico[a,b], L. Fiore[a], A. Gelmi[a,b], G. Iaselli[a,c], M. Ince[a,b], S. Lezki[a,b], G. Maggi[a,c], M. Maggi[a],
G. Miniello[a,b], S. My[a,b], S. Nuzzo[a,b], A. Pompili[a,b], G. Pugliese[a,c], R. Radogna[a], A. Ranieri[a], G. Selvaggi[a,b],
A. Sharma[a], L. Silvestris[a], R. Venditti[a], P. Verwilligen[a]

INFN Sezione di Bologna[a], Università di Bologna[b], Bologna, Italy
G. Abbiendi[a], C. Battilana[a,b], D. Bonacorsi[a,b], L. Borgonovi[a,b], S. Braibant-Giacomelli[a,b], R. Campanini[a,b],
P. Capiluppi[a,b], A. Castro[a,b], F. R. Cavallo[a], S. S. Chhibra[a,b], G. Codispoti[a,b], M. Cuffiani[a,b], G. M. Dallavalle[a],
F. Fabbri[a], A. Fanfani[a,b], E. Fontanesi, P. Giacomelli[a], C. Grandi[a], L. Guiducci[a,b], F. Iemmi[a,b], S. Lo Meo[a,29],
S. Marcellini[a], G. Masetti[a], A. Montanari[a], F. L. Navarria[a,b], A. Perrotta[a], F. Primavera[a,b], A. M. Rossi[a,b], T. Rovelli[a,b],
G. P. Siroli[a,b], N. Tosi[a]

INFN Sezione di Catania[a], Università di Catania[b], Catania, Italy
S. Albergo[a,b], A. Di Mattia[a], R. Potenza[a,b], A. Tricomi[a,b], C. Tuve[a,b]

INFN Sezione di Firenze[a], Università di Firenze[b], Florence, Italy
G. Barbagli[a], K. Chatterjee[a,b], V. Ciulli[a,b], C. Civinini[a], R. D'Alessandro[a,b], E. Focardi[a,b], G. Latino, P. Lenzi[a,b],
M. Meschini[a], S. Paoletti[a], L. Russo[a,30], G. Sguazzoni[a], D. Strom[a], L. Viliani[a]

INFN Laboratori Nazionali di Frascati, Frascati, Italy
L. Benussi, S. Bianco, F. Fabbri, D. Piccolo

INFN Sezione di Genova[a], Università di Genova[b], Genoa, Italy
F. Ferro[a], R. Mulargia[a,b], E. Robutti[a], S. Tosi[a,b]

INFN Sezione di Milano-Bicocca[a], Università di Milano-Bicocca[b], Milan, Italy
A. Benaglia[a], A. Beschi[b], F. Brivio[a,b], V. Ciriolo[a,b,16], S. Di Guida[a,b,16], M. E. Dinardo[a,b], S. Fiorendi[a,b], S. Gennai[a],
A. Ghezzi[a,b], P. Govoni[a,b], M. Malberti[a,b], S. Malvezzi[a], D. Menasce[a], F. Monti, L. Moroni[a], M. Paganoni[a,b],
D. Pedrini[a], S. Ragazzi[a,b], T. Tabarelli de Fatis[a,b], D. Zuolo[a,b]

INFN Sezione di Napoli[a], Università di Napoli 'Federico II'[b], Naples, Italy, Università della Basilicata[c], Potenza, Italy, Università G. Marconi[d], Rome, Italy
S. Buontempo[a], N. Cavallo[a,c], A. De Iorio[a,b], A. Di Crescenzo[a,b], F. Fabozzi[a,c], F. Fienga[a], G. Galati[a], A. O. M. Iorio[a,b],
W. A. Khan[a], L. Lista[a], S. Meola[a,d,16], P. Paolucci[a,16], C. Sciacca[a,b], E. Voevodina[a,b]

INFN Sezione di Padova[a], Università di Padova[b], Padova, Italy, Università di Trento[c], Trento, Italy
P. Azzi[a], N. Bacchetta[a], D. Bisello[a,b], A. Boletti[a,b], A. Bragagnolo, R. Carlin[a,b], P. Checchia[a], M. Dall'Osso[a,b], P. De Castro Manzano[a], T. Dorigo[a], U. Dosselli[a], F. Gasparini[a,b], U. Gasparini[a,b], A. Gozzelino[a], S. Y. Hoh, S. Lacaprara[a], P. Lujan, M. Margoni[a,b], A. T. Meneguzzo[a,b], J. Pazzini[a,b], M. Presilla[b], P. Ronchese[a,b], R. Rossin[a,b], F. Simonetto[a,b], A. Tiko, E. Torassa[a], M. Tosi[a,b], M. Zanetti[a,b], P. Zotto[a,b], G. Zumerle[a,b]

INFN Sezione di Pavia[a], Università di Pavia[b], Pavia, Italy
A. Braghieri[a], A. Magnani[a], P. Montagna[a,b], S. P. Ratti[a,b], V. Re[a], M. Ressegotti[a,b], C. Riccardi[a,b], P. Salvini[a], I. Vai[a,b], P. Vitulo[a,b]

INFN Sezione di Perugia[a], Università di Perugia[b], Perugia, Italy
M. Biasini[a,b], G. M. Bilei[a], C. Cecchi[a,b], D. Ciangottini[a,b], L. Fanò[a,b], P. Lariccia[a,b], R. Leonardi[a,b], E. Manoni[a], G. Mantovani[a,b], V. Mariani[a,b], M. Menichelli[a], A. Rossi[a,b], A. Santocchia[a,b], D. Spiga[a]

INFN Sezione di Pisa[a], Università di Pisa[b], Scuola Normale Superiore di Pisa[c], Pisa, Italy
K. Androsov[a], P. Azzurri[a], G. Bagliesi[a], L. Bianchini[a], T. Boccali[a], L. Borrello, R. Castaldi[a], M. A. Ciocci[a,b], R. Dell'Orso[a], G. Fedi[a], F. Fiori[a,c], L. Giannini[a,c], A. Giassi[a], M. T. Grippo[a], F. Ligabue[a,c], E. Manca[a,c], G. Mandorli[a,c], A. Messineo[a,b], F. Palla[a], A. Rizzi[a,b], G. Rolandi[31], P. Spagnolo[a], R. Tenchini[a], G. Tonelli[a,b], A. Venturi[a], P. G. Verdini[a]

INFN Sezione di Roma[a], Sapienza Università di Roma[b], Rome, Italy
L. Barone[a,b], F. Cavallari[a], M. Cipriani[a,b], D. Del Re[a,b], E. Di Marco[a,b], M. Diemoz[a], S. Gelli[a,b], E. Longo[a,b], B. Marzocchi[a,b], P. Meridiani[a], G. Organtini[a,b], F. Pandolfi[a], R. Paramatti[a,b], F. Preiato[a,b], S. Rahatlou[a,b], C. Rovelli[a], F. Santanastasio[a,b]

INFN Sezione di Torino[a], Università di Torino[b], Torino, Italy, Università del Piemonte Orientale[c], Novara, Italy
N. Amapane[a,b], R. Arcidiacono[a,c], S. Argiro[a,b], M. Arneodo[a,c], N. Bartosik[a], R. Bellan[a,b], C. Biino[a], A. Cappati[a,b], N. Cartiglia[a], F. Cenna[a,b], S. Cometti[a], M. Costa[a,b], R. Covarelli[a,b], N. Demaria[a], B. Kiani[a,b], C. Mariotti[a], S. Maselli[a], E. Migliore[a,b], V. Monaco[a,b], E. Monteil[a,b], M. Monteno[a], M. M. Obertino[a,b], L. Pacher[a,b], N. Pastrone[a], M. Pelliccioni[a], G. L. Pinna Angioni[a,b], A. Romero[a,b], M. Ruspa[a,c], R. Sacchi[a,b], R. Salvatico[a,b], K. Shchelina[a,b], V. Sola[a], A. Solano[a,b], D. Soldi[a,b], A. Staiano[a]

INFN Sezione di Trieste[a], Università di Trieste[b], Trieste, Italy
S. Belforte[a], V. Candelise[a,b], M. Casarsa[a], F. Cossutti[a], A. Da Rold[a,b], G. Della Ricca[a,b], F. Vazzoler[a,b], A. Zanetti[a]

Kyungpook National University, Daegu, Korea
D. H. Kim, G. N. Kim, M. S. Kim, J. Lee, S. Lee, S. W. Lee, C. S. Moon, Y. D. Oh, S. I. Pak, S. Sekmen, D. C. Son, Y. C. Yang

Institute for Universe and Elementary Particles, Chonnam National University, Kwangju, Korea
H. Kim, D. H. Moon, G. Oh

Hanyang University, Seoul, Korea
B. Francois, J. Goh[32], T. J. Kim

Korea University, Seoul, Korea
S. Cho, S. Choi, Y. Go, D. Gyun, S. Ha, B. Hong, Y. Jo, K. Lee, K. S. Lee, S. Lee, J. Lim, S. K. Park, Y. Roh

Sejong University, Seoul, Korea
H. S. Kim

Seoul National University, Seoul, Korea
J. Almond, J. Kim, J. S. Kim, H. Lee, K. Lee, K. Nam, S. B. Oh, B. C. Radburn-Smith, S. h. Seo, U. K. Yang, H. D. Yoo, G. B. Yu

University of Seoul, Seoul, Korea
D. Jeon, H. Kim, J. H. Kim, J. S. H. Lee, I. C. Park

Sungkyunkwan University, Suwon, Korea
Y. Choi, C. Hwang, J. Lee, I. Yu

Vilnius University, Vilnius, Lithuania
V. Dudenas, A. Juodagalvis, J. Vaitkus

National Centre for Particle Physics, Universiti Malaya, Kuala Lumpur, Malaysia
Z. A. Ibrahim, M. A. B. Md Ali[33], F. Mohamad Idris[34], W. A. T. Wan Abdullah, M. N. Yusli, Z. Zolkapli

Universidad de Sonora (UNISON), Hermosillo, Mexico
J. F. Benitez, A. Castaneda Hernandez, J. A. Murillo Quijada

Centro de Investigacion y de Estudios Avanzados del IPN, Mexico City, Mexico
H. Castilla-Valdez, E. De La Cruz-Burelo, M. C. Duran-Osuna, I. Heredia-De La Cruz[35], R. Lopez-Fernandez,
J. Mejia Guisao, R. I. Rabadan-Trejo, M. Ramirez-Garcia, G. Ramirez-Sanchez, R. Reyes-Almanza, A. Sanchez-Hernandez

Universidad Iberoamericana, Mexico City, Mexico
S. Carrillo Moreno, C. Oropeza Barrera, F. Vazquez Valencia

Benemerita Universidad Autonoma de Puebla, Puebla, Mexico
J. Eysermans, I. Pedraza, H. A. Salazar Ibarguen, C. Uribe Estrada

Universidad Autónoma de San Luis Potosí, San Luis Potosí, Mexico
A. Morelos Pineda

University of Auckland, Auckland, New Zealand
D. Krofcheck

University of Canterbury, Christchurch, New Zealand
S. Bheesette, P. H. Butler

National Centre for Physics, Quaid-I-Azam University, Islamabad, Pakistan
A. Ahmad, M. Ahmad, M. I. Asghar, Q. Hassan, H. R. Hoorani, A. Saddique, M. A. Shah, M. Shoaib, M. Waqas

National Centre for Nuclear Research, Swierk, Poland
H. Bialkowska, M. Bluj, B. Boimska, T. Frueboes, M. Górski, M. Kazana, M. Szleper, P. Traczyk, P. Zalewski

Institute of Experimental Physics, Faculty of Physics, University of Warsaw, Warsaw, Poland
K. Bunkowski, A. Byszuk[36], K. Doroba, A. Kalinowski, M. Konecki, J. Krolikowski, M. Misiura, M. Olszewski,
A. Pyskir, M. Walczak

Laboratório de Instrumentação e Física Experimental de Partículas, Lisbon, Portugal
M. Araujo, P. Bargassa, C. Beirão Da Cruz E Silva, A. Di Francesco, P. Faccioli, B. Galinhas, M. Gallinaro, J. Hollar,
N. Leonardo, J. Seixas, G. Strong, O. Toldaiev, J. Varela

Joint Institute for Nuclear Research, Dubna, Russia
S. Afanasiev, P. Bunin, M. Gavrilenko, I. Golutvin, I. Gorbunov, A. Kamenev, V. Karjavine, A. Lanev, A. Malakhov,
V. Matveev[37,38], P. Moisenz, V. Palichik, V. Perelygin, S. Shmatov, S. Shulha, N. Skatchkov, V. Smirnov, N. Voytishin,
A. Zarubin

Petersburg Nuclear Physics Institute, Gatchina (St. Petersburg), Russia
V. Golovtsov, Y. Ivanov, V. Kim[39], E. Kuznetsova[40], P. Levchenko, V. Murzin, V. Oreshkin, I. Smirnov, D. Sosnov,
V. Sulimov, L. Uvarov, S. Vavilov, A. Vorobyev

Institute for Nuclear Research, Moscow, Russia
Yu. Andreev, A. Dermenev, S. Gninenko, N. Golubev, A. Karneyeu, M. Kirsanov, N. Krasnikov, A. Pashenkov,
A. Shabanov, D. Tlisov, A. Toropin

Institute for Theoretical and Experimental Physics, Moscow, Russia
V. Epshteyn, V. Gavrilov, N. Lychkovskaya, V. Popov, I. Pozdnyakov, G. Safronov, A. Spiridonov, A. Stepennov,
V. Stolin, M. Toms, E. Vlasov, A. Zhokin

Moscow Institute of Physics and Technology, Moscow, Russia
T. Aushev

National Research Nuclear University 'Moscow Engineering Physics Institute' (MEPhI), Moscow, Russia
R. Chistov[41], M. Danilov[41], P. Parygin, E. Tarkovskii, V. Rusinov

P.N. Lebedev Physical Institute, Moscow, Russia
V. Andreev, M. Azarkin, I. Dremin[38], M. Kirakosyan, A. Terkulov

Skobeltsyn Institute of Nuclear Physics, Lomonosov Moscow State University, Moscow, Russia
A. Baskakov, A. Belyaev, E. Boos, V. Bunichev, M. Dubinin[42], L. Dudko, A. Gribushin, V. Klyukhin, O. Kodolova,
I. Lokhtin, I. Miagkov, S. Obraztsov, M. Perfilov, S. Petrushanko, V. Savrin

Novosibirsk State University (NSU), Novosibirsk, Russia
A. Barnyakov[43], V. Blinov[43], T. Dimova[43], L. Kardapoltsev[43], Y. Skovpen[43]

Institute for High Energy Physics of National Research Centre 'Kurchatov Institute', Protvino, Russia
I. Azhgirey, I. Bayshev, S. Bitioukov, V. Kachanov, A. Kalinin, D. Konstantinov, P. Mandrik, V. Petrov, R. Ryutin,
S. Slabospitskii, A. Sobol, S. Troshin, N. Tyurin, A. Uzunian, A. Volkov

National Research Tomsk Polytechnic University, Tomsk, Russia
A. Babaev, S. Baidali, V. Okhotnikov

Faculty of Physics and Vinca Institute of Nuclear Sciences, University of Belgrade, Belgrade, Serbia
P. Adzic[44], P. Cirkovic, D. Devetak, M. Dordevic, J. Milosevic

Centro de Investigaciones Energéticas Medioambientales y Tecnológicas (CIEMAT), Madrid, Spain
J. Alcaraz Maestre, A. Álvarez Fernández, I. Bachiller, M. Barrio Luna, J. A. Brochero Cifuentes, M. Cerrada, N. Colino,
B. De La Cruz, A. Delgado Peris, C. Fernandez Bedoya, J. P. Fernández Ramos, J. Flix, M. C. Fouz, O. Gonzalez Lopez,
S. Goy Lopez, J. M. Hernandez, M. I. Josa, D. Moran, A. Pérez-Calero Yzquierdo, J. Puerta Pelayo, I. Redondo,
L. Romero, S. Sánchez Navas, M. S. Soares, A. Triossi

Universidad Autónoma de Madrid, Madrid, Spain
C. Albajar, J. F. de Trocóniz

Universidad de Oviedo, Oviedo, Spain
J. Cuevas, C. Erice, J. Fernandez Menendez, S. Folgueras, I. Gonzalez Caballero, J. R. González Fernández,
E. Palencia Cortezon, V. Rodríguez Bouza, S. Sanchez Cruz, J. M. Vizan Garcia

Instituto de Física de Cantabria (IFCA), CSIC-Universidad de Cantabria, Santander, Spain
I. J. Cabrillo, A. Calderon, B. Chazin Quero, J. Duarte Campderros, M. Fernandez, P. J. Fernández Manteca,
A. García Alonso, J. Garcia-Ferrero, G. Gomez, A. Lopez Virto, J. Marco, C. Martinez Rivero, P. Martinez Ruiz del Arbol,
F. Matorras, J. Piedra Gomez, C. Prieels, T. Rodrigo, A. Ruiz-Jimeno, L. Scodellaro, N. Trevisani, I. Vila,
R. Vilar Cortabitarte

Department of Physics, University of Ruhuna, Matara, Sri Lanka
N. Wickramage

CERN, European Organization for Nuclear Research, Geneva, Switzerland
D. Abbaneo, B. Akgun, E. Auffray, G. Auzinger, P. Baillon, A. H. Ball, D. Barney, J. Bendavid, M. Bianco, A. Bocci,
C. Botta, E. Brondolin, T. Camporesi, M. Cepeda, G. Cerminara, E. Chapon, Y. Chen, G. Cucciati, D. d'Enterria,
A. Dabrowski, N. Daci, V. Daponte, A. David, A. De Roeck, N. Deelen, M. Dobson, M. Dünser, N. Dupont,
A. Elliott-Peisert, P. Everaerts, F. Fallavollita[45], D. Fasanella, G. Franzoni, J. Fulcher, W. Funk, D. Gigi, A. Gilbert,
K. Gill, F. Glege, M. Gruchala, M. Guilbaud, D. Gulhan, J. Hegeman, C. Heidegger, V. Innocente, A. Jafari, P. Janot,
O. Karacheban[19], J. Kieseler, A. Kornmayer, M. Krammer[1], C. Lange, P. Lecoq, C. Lourenço, L. Malgeri, M. Mannelli,
A. Massironi, F. Meijers, J. A. Merlin, S. Mersi, E. Meschi, P. Milenovic[46], F. Moortgat, M. Mulders, J. Ngadiuba,
S. Nourbakhsh, S. Orfanelli, L. Orsini, F. Pantaleo[16], L. Pape, E. Perez, M. Peruzzi, A. Petrilli, G. Petrucciani, A. Pfeiffer,
M. Pierini, F. M. Pitters, D. Rabady, A. Racz, T. Reis, M. Rovere, H. Sakulin, C. Schäfer, C. Schwick, M. Selvaggi,
A. Sharma, P. Silva, P. Sphicas[47], A. Stakia, J. Steggemann, D. Treille, A. Tsirou, A. Vartak, V. Veckalns[48], M. Verzetti,
W. D. Zeuner

Paul Scherrer Institut, Villigen, Switzerland
L. Caminada[49], K. Deiters, W. Erdmann, R. Horisberger, Q. Ingram, H. C. Kaestli, D. Kotlinski, U. Langenegger, T. Rohe, S. A. Wiederkehr

ETH Zurich-Institute for Particle Physics and Astrophysics (IPA), Zurich, Switzerland
M. Backhaus, L. Bäni, P. Berger, N. Chernyavskaya, G. Dissertori, M. Dittmar, M. Donegà, C. Dorfer, T. A. Gómez Espinosa, C. Grab, D. Hits, T. Klijnsma, W. Lustermann, R. A. Manzoni, M. Marionneau, M. T. Meinhard, F. Micheli, P. Musella, F. Nessi-Tedaldi, F. Pauss, G. Perrin, L. Perrozzi, S. Pigazzini, C. Reissel, D. Ruini, D. A. Sanz Becerra, M. Schönenberger, L. Shchutska, V. R. Tavolaro, K. Theofilatos, M. L. Vesterbacka Olsson, R. Wallny, D. H. Zhu

Universität Zürich, Zurich, Switzerland
T. K. Aarrestad, C. Amsler[50], D. Brzhechko, M. F. Canelli, A. De Cosa, R. Del Burgo, S. Donato, C. Galloni, T. Hreus, B. Kilminster, S. Leontsinis, I. Neutelings, G. Rauco, P. Robmann, D. Salerno, K. Schweiger, C. Seitz, Y. Takahashi, A. Zucchetta

National Central University, Chung-Li, Taiwan
T. H. Doan, R. Khurana, C. M. Kuo, W. Lin, A. Pozdnyakov, S. S. Yu

National Taiwan University (NTU), Taipei, Taiwan
P. Chang, Y. Chao, K. F. Chen, P. H. Chen, W.-S. Hou, Y. F. Liu, R.-S. Lu, E. Paganis, A. Psallidas, A. Steen

Faculty of Science, Department of Physics, Chulalongkorn University, Bangkok, Thailand
B. Asavapibhop, N. Srimanobhas, N. Suwonjandee

Physics Department, Science and Art Faculty, Çukurova University, Adana, Turkey
A. Bat, F. Boran, S. Cerci[51], S. Damarseckin, Z. S. Demiroglu, F. Dolek, C. Dozen, I. Dumanoglu, G. Gokbulut, Y. Guler, E. Gurpinar, I. Hos[52], C. Isik, E. E. Kangal[53], O. Kara, A. Kayis Topaksu, U. Kiminsu, M. Oglakci, G. Onengut, K. Ozdemir[54], S. Ozturk[55], D. Sunar Cerci[51], B. Tali[51], U. G. Tok, S. Turkcapar, I. S. Zorbakir, C. Zorbilmez

Physics Department, Middle East Technical University, Ankara, Turkey
B. Isildak[56], G. Karapinar[57], M. Yalvac, M. Zeyrek

Bogazici University, Istanbul, Turkey
I. O. Atakisi, E. Gülmez, M. Kaya[58], O. Kaya[59], S. Ozkorucuklu[60], S. Tekten, E. A. Yetkin[61]

Istanbul Technical University, Istanbul, Turkey
M. N. Agaras, A. Cakir, K. Cankocak, Y. Komurcu, S. Sen[62]

Institute for Scintillation Materials of National Academy of Science of Ukraine, Kharkov, Ukraine
B. Grynyov

National Scientific Center, Kharkov Institute of Physics and Technology, Kharkov, Ukraine
L. Levchuk

University of Bristol, Bristol, UK
F. Ball, J. J. Brooke, D. Burns, E. Clement, D. Cussans, O. Davignon, H. Flacher, J. Goldstein, G. P. Heath, H. F. Heath, L. Kreczko, D. M. Newbold[63], S. Paramesvaran, B. Penning, T. Sakuma, D. Smith, V. J. Smith, J. Taylor, A. Titterton

Rutherford Appleton Laboratory, Didcot, UK
K. W. Bell, A. Belyaev[64], C. Brew, R. M. Brown, D. Cieri, D. J. A. Cockerill, J. A. Coughlan, K. Harder, S. Harper, J. Linacre, K. Manolopoulos, E. Olaiya, D. Petyt, C. H. Shepherd-Themistocleous, A. Thea, I. R. Tomalin, T. Williams, W. J. Womersley

Imperial College, London, UK
R. Bainbridge, P. Bloch, J. Borg, S. Breeze, O. Buchmuller, A. Bundock, D. Colling, P. Dauncey, G. Davies, M. Della Negra, R. Di Maria, G. Hall, G. Iles, T. James, M. Komm, L. Lyons, A.-M. Magnan, S. Malik, A. Martelli, J. Nash[65], A. Nikitenko[7], V. Palladino, M. Pesaresi, D. M. Raymond, A. Richards, A. Rose, E. Scott, C. Seez, A. Shtipliyski, G. Singh, M. Stoye, T. Strebler, S. Summers, A. Tapper, K. Uchida, T. Virdee[16], N. Wardle, D. Winterbottom, S. C. Zenz

Brunel University, Uxbridge, UK

J. E. Cole, P. R. Hobson, A. Khan, P. Kyberd, C. K. Mackay, A. Morton, I. D. Reid, L. Teodorescu, S. Zahid

Baylor University, Waco, USA

K. Call, J. Dittmann, K. Hatakeyama, H. Liu, C. Madrid, B. McMaster, N. Pastika, C. Smith

Catholic University of America, Washington, DC, USA

R. Bartek, A. Dominguez

The University of Alabama, Tuscaloosa, USA

A. Buccilli, S. I. Cooper, C. Henderson, P. Rumerio, C. West

Boston University, Boston, USA

D. Arcaro, T. Bose, D. Gastler, S. Girgis, D. Pinna, D. Rankin, C. Richardson, J. Rohlf, L. Sulak, D. Zou

Brown University, Providence, USA

G. Benelli, X. Coubez, D. Cutts, M. Hadley, J. Hakala, U. Heintz, J. M. Hogan[66], K. H. M. Kwok, E. Laird, G. Landsberg, J. Lee, Z. Mao, M. Narain, S. Sagir[67], R. Syarif, E. Usai, D. Yu

University of California, Davis, Davis, USA

R. Band, C. Brainerd, R. Breedon, D. Burns, M. Calderon De La Barca Sanchez, M. Chertok, J. Conway, R. Conway, P. T. Cox, R. Erbacher, C. Flores, G. Funk, W. Ko, O. Kukral, R. Lander, M. Mulhearn, D. Pellett, J. Pilot, S. Shalhout, M. Shi, D. Stolp, D. Taylor, K. Tos, M. Tripathi, Z. Wang, F. Zhang

University of California, Los Angeles, USA

M. Bachtis, C. Bravo, R. Cousins, A. Dasgupta, A. Florent, J. Hauser, M. Ignatenko, N. Mccoll, S. Regnard, D. Saltzberg, C. Schnaible, V. Valuev

University of California, Riverside, Riverside, USA

E. Bouvier, K. Burt, R. Clare, J. W. Gary, S. M. A. Ghiasi Shirazi, G. Hanson, G. Karapostoli, E. Kennedy, F. Lacroix, O. R. Long, M. Olmedo Negrete, M. I. Paneva, W. Si, L. Wang, H. Wei, S. Wimpenny, B. R. Yates

University of California, San Diego, La Jolla, USA

J. G. Branson, P. Chang, S. Cittolin, M. Derdzinski, R. Gerosa, D. Gilbert, B. Hashemi, A. Holzner, D. Klein, G. Kole, V. Krutelyov, J. Letts, M. Masciovecchio, D. Olivito, S. Padhi, M. Pieri, M. Sani, V. Sharma, S. Simon, M. Tadel, J. Wood, F. Würthwein, A. Yagil, G. Zevi Della Porta

Department of Physics, University of California, Santa Barbara, Santa Barbara, USA

N. Amin, R. Bhandari, C. Campagnari, M. Citron, V. Dutta, M. Franco Sevilla, L. Gouskos, R. Heller, J. Incandela, H. Mei, A. Ovcharova, H. Qu, J. Richman, D. Stuart, I. Suarez, S. Wang, J. Yoo

California Institute of Technology, Pasadena, USA

D. Anderson, A. Bornheim, J. M. Lawhorn, N. Lu, H. B. Newman, T. Q. Nguyen, J. Pata, M. Spiropulu, J. R. Vlimant, R. Wilkinson, S. Xie, Z. Zhang, R. Y. Zhu

Carnegie Mellon University, Pittsburgh, USA

M. B. Andrews, T. Ferguson, T. Mudholkar, M. Paulini, M. Sun, I. Vorobiev, M. Weinberg

University of Colorado Boulder, Boulder, USA

J. P. Cumalat, W. T. Ford, F. Jensen, A. Johnson, E. MacDonald, T. Mulholland, R. Patel, A. Perloff, K. Stenson, K. A. Ulmer, S. R. Wagner

Cornell University, Ithaca, USA

J. Alexander, J. Chaves, Y. Cheng, J. Chu, A. Datta, K. Mcdermott, N. Mirman, J. R. Patterson, D. Quach, A. Rinkevicius, A. Ryd, L. Skinnari, L. Soffi, S. M. Tan, Z. Tao, J. Thom, J. Tucker, P. Wittich, M. Zientek

Fermi National Accelerator Laboratory, Batavia, USA

S. Abdullin, M. Albrow, M. Alyari, G. Apollinari, A. Apresyan, A. Apyan, S. Banerjee, L. A. T. Bauerdick, A. Beretvas, J. Berryhill, P. C. Bhat, K. Burkett, J. N. Butler, A. Canepa, G. B. Cerati, H. W. K. Cheung, F. Chlebana, M. Cremonesi, J. Duarte, V. D. Elvira, J. Freeman, Z. Gecse, E. Gottschalk, L. Gray, D. Green, S. Grünendahl, O. Gutsche, J. Hanlon,

R. M. Harris, S. Hasegawa, J. Hirschauer, Z. Hu, B. Jayatilaka, S. Jindariani, M. Johnson, U. Joshi, B. Klima,
M. J. Kortelainen, B. Kreis, S. Lammel, D. Lincoln, R. Lipton, M. Liu, T. Liu, J. Lykken, K. Maeshima, J. M. Marraffino,
D. Mason, P. McBride, P. Merkel, S. Mrenna, S. Nahn, V. O'Dell, K. Pedro, C. Pena, O. Prokofyev, G. Rakness, F. Ravera,
A. Reinsvold, L. Ristori, A. Savoy-Navarro[68], B. Schneider, E. Sexton-Kennedy, A. Soha, W. J. Spalding, L. Spiegel,
S. Stoynev, J. Strait, N. Strobbe, L. Taylor, S. Tkaczyk, N. V. Tran, L. Uplegger, E. W. Vaandering, C. Vernieri,
M. Verzocchi, R. Vidal, M. Wang, H. A. Weber, A. Whitbeck

University of Florida, Gainesville, USA
D. Acosta, P. Avery, P. Bortignon, D. Bourilkov, A. Brinkerhoff, L. Cadamuro, A. Carnes, D. Curry, R. D. Field,
S. V. Gleyzer, B. M. Joshi, J. Konigsberg, A. Korytov, K. H. Lo, P. Ma, K. Matchev, G. Mitselmakher, D. Rosenzweig,
K. Shi, D. Sperka, J. Wang, S. Wang, X. Zuo

Florida International University, Miami, USA
Y. R. Joshi, S. Linn

Florida State University, Tallahassee, USA
A. Ackert, T. Adams, A. Askew, S. Hagopian, V. Hagopian, K. F. Johnson, T. Kolberg, G. Martinez, T. Perry, H. Prosper,
A. Saha, C. Schiber, R. Yohay

Florida Institute of Technology, Melbourne, USA
M. M. Baarmand, V. Bhopatkar, S. Colafranceschi, M. Hohlmann, D. Noonan, M. Rahmani, T. Roy, F. Yumiceva

University of Illinois at Chicago (UIC), Chicago, USA
M. R. Adams, L. Apanasevich, D. Berry, R. R. Betts, R. Cavanaugh, X. Chen, S. Dittmer, O. Evdokimov, C. E. Gerber,
D. A. Hangal, D. J. Hofman, K. Jung, J. Kamin, C. Mills, M. B. Tonjes, N. Varelas, H. Wang, X. Wang, Z. Wu, J. Zhang

The University of Iowa, Iowa City, USA
M. Alhusseini, B. Bilki[69], W. Clarida, K. Dilsiz[70], S. Durgut, R. P. Gandrajula, M. Haytmyradov, V. Khristenko,
J.-P. Merlo, A. Mestvirishvili, A. Moeller, J. Nachtman, H. Ogul[71], Y. Onel, F. Ozok[72], A. Penzo, C. Snyder, E. Tiras,
J. Wetzel

Johns Hopkins University, Baltimore, USA
B. Blumenfeld, A. Cocoros, N. Eminizer, D. Fehling, L. Feng, A. V. Gritsan, W. T. Hung, P. Maksimovic, J. Roskes,
U. Sarica, M. Swartz, M. Xiao

The University of Kansas, Lawrence, USA
A. Al-bataineh, P. Baringer, A. Bean, S. Boren, J. Bowen, A. Bylinkin, J. Castle, S. Khalil, A. Kropivnitskaya,
D. Majumder, W. Mcbrayer, M. Murray, C. Rogan, S. Sanders, E. Schmitz, J. D. Tapia Takaki, Q. Wang

Kansas State University, Manhattan, USA
S. Duric, A. Ivanov, K. Kaadze, D. Kim, Y. Maravin, D. R. Mendis, T. Mitchell, A. Modak, A. Mohammadi

Lawrence Livermore National Laboratory, Livermore, USA
F. Rebassoo, D. Wright

University of Maryland, College Park, USA
A. Baden, O. Baron, A. Belloni, S. C. Eno, Y. Feng, C. Ferraioli, N. J. Hadley, S. Jabeen, G. Y. Jeng, R. G. Kellogg,
J. Kunkle, A. C. Mignerey, S. Nabili, F. Ricci-Tam, M. Seidel, Y. H. Shin, A. Skuja, S. C. Tonwar, K. Wong

Massachusetts Institute of Technology, Cambridge, USA
D. Abercrombie, B. Allen, V. Azzolini, A. Baty, G. Bauer, R. Bi, S. Brandt, W. Busza, I. A. Cali, M. D'Alfonso,
Z. Demiragli, G. Gomez Ceballos, M. Goncharov, P. Harris, D. Hsu, M. Hu, Y. Iiyama, G. M. Innocenti, M. Klute,
D. Kovalskyi, Y.-J. Lee, P. D. Luckey, B. Maier, A. C. Marini, C. Mcginn, C. Mironov, S. Narayanan, X. Niu, C. Paus,
C. Roland, G. Roland, Z. Shi, G. S. F. Stephans, K. Sumorok, K. Tatar, D. Velicanu, J. Wang, T. W. Wang, B. Wyslouch

University of Minnesota, Minneapolis, USA
A. C. Benvenuti[†], R. M. Chatterjee, A. Evans, P. Hansen, J. Hiltbrand, Sh. Jain, S. Kalafut, M. Krohn, Y. Kubota, Z. Lesko,
J. Mans, N. Ruckstuhl, R. Rusack, M. A. Wadud

University of Mississippi, Oxford, USA
J. G. Acosta, S. Oliveros

University of Nebraska-Lincoln, Lincoln, USA
E. Avdeeva, K. Bloom, D. R. Claes, C. Fangmeier, F. Golf, R. Gonzalez Suarez, R. Kamalieddin, I. Kravchenko, J. Monroy, J. E. Siado, G. R. Snow, B. Stieger

State University of New York at Buffalo, Buffalo, USA
A. Godshalk, C. Harrington, I. Iashvili, A. Kharchilava, C. Mclean, D. Nguyen, A. Parker, S. Rappoccio, B. Roozbahani

Northeastern University, Boston, USA
G. Alverson, E. Barberis, C. Freer, Y. Haddad, A. Hortiangtham, D. M. Morse, T. Orimoto, T. Wamorkar, B. Wang, A. Wisecarver, D. Wood

Northwestern University, Evanston, USA
S. Bhattacharya, J. Bueghly, O. Charaf, T. Gunter, K. A. Hahn, N. Odell, M. H. Schmitt, K. Sung, M. Trovato, M. Velasco

University of Notre Dame, Notre Dame, USA
R. Bucci, N. Dev, M. Hildreth, K. Hurtado Anampa, C. Jessop, D. J. Karmgard, K. Lannon, W. Li, N. Loukas, N. Marinelli, F. Meng, C. Mueller, Y. Musienko[37], M. Planer, R. Ruchti, P. Siddireddy, G. Smith, S. Taroni, M. Wayne, A. Wightman, M. Wolf, A. Woodard

The Ohio State University, Columbus, USA
J. Alimena, L. Antonelli, B. Bylsma, L. S. Durkin, S. Flowers, B. Francis, C. Hill, W. Ji, T. Y. Ling, W. Luo, B. L. Winer

Princeton University, Princeton, USA
S. Cooperstein, P. Elmer, J. Hardenbrook, N. Haubrich, S. Higginbotham, A. Kalogeropoulos, S. Kwan, D. Lange, M. T. Lucchini, J. Luo, D. Marlow, K. Mei, I. Ojalvo, J. Olsen, C. Palmer, P. Piroué, J. Salfeld-Nebgen, D. Stickland, C. Tully

University of Puerto Rico, Mayagüez, USA
S. Malik, S. Norberg

Purdue University, West Lafayette, USA
A. Barker, V. E. Barnes, S. Das, L. Gutay, M. Jones, A. W. Jung, A. Khatiwada, B. Mahakud, D. H. Miller, N. Neumeister, C. C. Peng, S. Piperov, H. Qiu, J. F. Schulte, J. Sun, F. Wang, R. Xiao, W. Xie

Purdue University Northwest, Hammond, USA
T. Cheng, J. Dolen, N. Parashar

Rice University, Houston, USA
Z. Chen, K. M. Ecklund, S. Freed, F. J. M. Geurts, M. Kilpatrick, Arun Kumar, W. Li, B. P. Padley, R. Redjimi, J. Roberts, J. Rorie, W. Shi, Z. Tu, A. Zhang

University of Rochester, Rochester, USA
A. Bodek, P. de Barbaro, R. Demina, Y. t. Duh, J. L. Dulemba, C. Fallon, T. Ferbel, M. Galanti, A. Garcia-Bellido, J. Han, O. Hindrichs, A. Khukhunaishvili, E. Ranken, P. Tan, R. Taus

Rutgers, The State University of New Jersey, Piscataway, USA
B. Chiarito, J. P. Chou, Y. Gershtein, E. Halkiadakis, A. Hart, M. Heindl, E. Hughes, S. Kaplan, R. Kunnawalkam Elayavalli, S. Kyriacou, I. Laflotte, A. Lath, R. Montalvo, K. Nash, M. Osherson, H. Saka, S. Salur, S. Schnetzer, D. Sheffield, S. Somalwar, R. Stone, S. Thomas, P. Thomassen

University of Tennessee, Knoxville, USA
A. G. Delannoy, J. Heideman, G. Riley, S. Spanier

Texas A&M University, College Station, USA
O. Bouhali[73], A. Celik, M. Dalchenko, M. De Mattia, A. Delgado, S. Dildick, R. Eusebi, J. Gilmore, T. Huang, T. Kamon[74], S. Luo, D. Marley, R. Mueller, D. Overton, L. Perniè, D. Rathjens, A. Safonov

Texas Tech University, Lubbock, USA

N. Akchurin, J. Damgov, F. De Guio, P. R. Dudero, S. Kunori, K. Lamichhane, S. W. Lee, T. Mengke, S. Muthumuni, T. Peltola, S. Undleeb, I. Volobouev, Z. Wang

Vanderbilt University, Nashville, USA

S. Greene, A. Gurrola, R. Janjam, W. Johns, C. Maguire, A. Melo, H. Ni, K. Padeken, F. Romeo, J. D. Ruiz Alvarez, P. Sheldon, S. Tuo, J. Velkovska, M. Verweij, Q. Xu

University of Virginia, Charlottesville, USA

M. W. Arenton, P. Barria, B. Cox, R. Hirosky, M. Joyce, A. Ledovskoy, H. Li, C. Neu, T. Sinthuprasith, Y. Wang, E. Wolfe, F. Xia

Wayne State University, Detroit, USA

R. Harr, P. E. Karchin, N. Poudyal, J. Sturdy, P. Thapa, S. Zaleski

University of Wisconsin - Madison, Madison, WI, USA

J. Buchanan, C. Caillol, D. Carlsmith, S. Dasu, I. De Bruyn, L. Dodd, B. Gomber[75], M. Grothe, M. Herndon, A. Hervé, U. Hussain, P. Klabbers, A. Lanaro, K. Long, R. Loveless, T. Ruggles, A. Savin, V. Sharma, N. Smith, W. H. Smith, N. Woods

† **Deceased**

1: Also at Vienna University of Technology, Vienna, Austria
2: Also at IRFU, CEA, Université Paris-Saclay, Gif-sur-Yvette, France
3: Also at Universidade Estadual de Campinas, Campinas, Brazil
4: Also at Federal University of Rio Grande do Sul, Porto Alegre, Brazil
5: Also at Université Libre de Bruxelles, Brussels, Belgium
6: Also at University of Chinese Academy of Sciences, Beijing, China
7: Also at Institute for Theoretical and Experimental Physics, Moscow, Russia
8: Also at Joint Institute for Nuclear Research, Dubna, Russia
9: Now at Helwan University, Cairo, Egypt
10: Also at Zewail City of Science and Technology, Zewail, Egypt
11: Now at Fayoum University, El-Fayoum, Egypt
12: Also at Department of Physics, King Abdulaziz University, Jeddah, Saudi Arabia
13: Also at Université de Haute Alsace, Mulhouse, France
14: Also at Skobeltsyn Institute of Nuclear Physics, Lomonosov Moscow State University, Moscow, Russia
15: Also at Tbilisi State University, Tbilisi, Georgia
16: Also at CERN, European Organization for Nuclear Research, Geneva, Switzerland
17: Also at RWTH Aachen University, III. Physikalisches Institut A, Aachen, Germany
18: Also at University of Hamburg, Hamburg, Germany
19: Also at Brandenburg University of Technology, Cottbus, Germany
20: Also at Institute of Physics, University of Debrecen, Debrecen, Hungary
21: Also at Institute of Nuclear Research ATOMKI, Debrecen, Hungary
22: Also at MTA-ELTE Lendület CMS Particle and Nuclear Physics Group, Eötvös Loránd University, Budapest, Hungary
23: Also at Indian Institute of Technology Bhubaneswar, Bhubaneswar, India
24: Also at Institute of Physics, Bhubaneswar, India
25: Also at Shoolini University, Solan, India
26: Also at University of Visva-Bharati, Santiniketan, India
27: Also at Isfahan University of Technology, Isfahan, Iran
28: Also at Plasma Physics Research Center, Science and Research Branch, Islamic Azad University, Tehran, Iran
29: Also at Italian National Agency for New Technologies, Energy and Sustainable Economic Development, Bologna, Italy
30: Also at Università degli Studi di Siena, Siena, Italy
31: Also at Scuola Normale e Sezione dell'INFN, Pisa, Italy
32: Also at Kyunghee University, Seoul, Korea
33: Also at International Islamic University of Malaysia, Kuala Lumpur, Malaysia
34: Also at Malaysian Nuclear Agency, MOSTI, Kajang, Malaysia

35: Also at Consejo Nacional de Ciencia y Tecnología, Mexico City, Mexico

36: Also at Warsaw University of Technology, Institute of Electronic Systems, Warsaw, Poland

37: Also at Institute for Nuclear Research, Moscow, Russia

38: Now at National Research Nuclear University 'Moscow Engineering Physics Institute' (MEPhI), Moscow, Russia

39: Also at St. Petersburg State Polytechnical University, St. Petersburg, Russia

40: Also at University of Florida, Gainesville, USA

41: Also at P.N. Lebedev Physical Institute, Moscow, Russia

42: Also at California Institute of Technology, Pasadena, USA

43: Also at Budker Institute of Nuclear Physics, Novosibirsk, Russia

44: Also at Faculty of Physics, University of Belgrade, Belgrade, Serbia

45: Also at INFN Sezione di Pavia^a, Università di Pavia^b, Pavia, Italy

46: Also at University of Belgrade, Faculty of Physics and Vinca Institute of Nuclear Sciences, Belgrade, Serbia

47: Also at National and Kapodistrian University of Athens, Athens, Greece

48: Also at Riga Technical University, Riga, Latvia

49: Also at Universität Zürich, Zurich, Switzerland

50: Also at Stefan Meyer Institute for Subatomic Physics (SMI), Vienna, Austria

51: Also at Adiyaman University, Adiyaman, Turkey

52: Also at Istanbul Aydin University, Istanbul, Turkey

53: Also at Mersin University, Mersin, Turkey

54: Also at Piri Reis University, Istanbul, Turkey

55: Also at Gaziosmanpasa University, Tokat, Turkey

56: Also at Ozyegin University, Istanbul, Turkey

57: Also at Izmir Institute of Technology, Izmir, Turkey

58: Also at Marmara University, Istanbul, Turkey

59: Also at Kafkas University, Kars, Turkey

60: Also at Istanbul University, Faculty of Science, Istanbul, Turkey

61: Also at Istanbul Bilgi University, Istanbul, Turkey

62: Also at Hacettepe University, Ankara, Turkey

63: Also at Rutherford Appleton Laboratory, Didcot, UK

64: Also at School of Physics and Astronomy, University of Southampton, Southampton, UK

65: Also at Monash University, Faculty of Science, Clayton, Australia

66: Also at Bethel University, St. Paul, USA

67: Also at Karamanoğlu Mehmetbey University, Karaman, Turkey

68: Also at Purdue University, West Lafayette, USA

69: Also at Beykent University, Istanbul, Turkey

70: Also at Bingol University, Bingol, Turkey

71: Also at Sinop University, Sinop, Turkey

72: Also at Mimar Sinan University, Istanbul, Istanbul, Turkey

73: Also at Texas A&M University at Qatar, Doha, Qatar

74: Also at Kyungpook National University, Daegu, Korea

75: Also at University of Hyderabad, Hyderabad, India